A coupled longitudinal-transverse nonlinear NSGT model for CNTs incorporating internal energy loss

Mergen H. Ghayesh [a], Hamed Farokhi [b], Ali Farajpour [a*]

[a] *School of Mechanical Engineering, University of Adelaide, South Australia 5005, Australia,*
Email: mergen.ghayesh@adelaide.edu.au (M.H. Ghayesh)
[*] *Corresponding author: ali.farajpourouderji@adelaide.edu.au, (A. Farajpour)*
[b] *Department of Mechanical and Construction Engineering,*
Northumbria University, Newcastle upon Tyne NE1 8ST, UK
Email: hamed.farokhi@northumbria.ac.uk (H. Farokhi)

Abstract

The aim of the present study is to comprehensively analyse scale effects on the mechanical characteristics of carbon nanotubes (CNTs) with viscoelastic properties. A scale-dependent coupled longitudinal-transverse nonlinear formulation is presented for this aim. The role of both the longitudinal and transverse motions as well as the viscosity effect due to the internal loss of the total energy are taken into account. The influence of large deformations due to the geometric nonlinearity is also taken into account. The nonlocal strain gradient theory (NSGT) is applied so as to describe scale effects on the mechanical characteristics of viscoelastic CNTs. Compared to the classical nonlocal theory, the NSGT better estimates scale effects since it is able to describe both the stiffness-hardening and –softening behaviours. The Kelvin–Voigt approach is used to capture the influence of the internal energy loss. Application of the NSGT together with the Hamilton principle yields the energy potential, the external work and the coupled longitudinal-transverse equations of the CNT. To determine an accurate numerical solution, the Galerkin scheme of discretisation and a continuation approach are finally utilised. The role of different parameters of the nanosystem in the nonlinear coupled mechanics of viscoelastic CNTs is discussed.

Keywords: Coupled longitudinal-transverse motion, Viscoelastic CNTs; Nonlinear mechanics; Nonlocal strain gradient model

1. Introduction

Carbon nanotubes (CNTs) have many promising applications in microelectromechanical and nanoelectromechanical systems (MEMSs and NEMSs) due to their unique electrical and mechanical features. In order to apply them properly in some ultrasmall devices such as nanoelectromechanical sensors and resonators, their time-dependent deformation under mechanical stresses should be investigated first.

In addition to experimental techniques, some theoretical models have been developed to estimate the mechanical behaviour of CNTs. A refined theoretical model for these valuable ultrasmall structures should be size-dependent since size effects have been proven to be significant at nanoscale levels. Furthermore, the model should include the influence of internal friction due to the fact that CNTs possess viscoelastic properties [1]. In the present study, the Kelvin–Voigt scheme is employed to describe the effect of internal dissipation.

A considerable number of size-dependent theoretical formulations have been proposed to extract the mechanical response of both microscale and nanoscale structures. For example, Setoodeh et al. [2] utilised a nonlocal Mindlin theory of plates to extract the nonlinear vibration response of graphene sheets. Moreover, Beni and Malekzadeh [3] examined the nonlinear vibration of non-prismatic skew nanoscale plates using a nonlocal formulation. In another investigation reported in Ref. [4], scale effects on the vibration of short nanoscale tubes surrounded by an elastic matrix were investigated. In addition, a nonlocal model with surface effects [5], a nonlocal two-variable refined model [6] and a nonlocal model with piezoelectric effects [7] have been developed for the vibration of nanoscale plates.

Some theoretical analyses have been performed on the mechanical characteristics of carbon nanotubes and nanobeams [8] since the invention of carbon nanotubes in 1991 [9]. For example, theoretical formulations have been developed for the postbuckling of smart composite nanotubes [10], wave propagations in nonlocal beams [11], vibrations of functionally graded nanobeams [12] and flexoelectric nanobeams [13]. In addition, various scale-edependent advanced models such as the classical [14], stress-driven [15] and higher-order [16] versions of nonlocal strain gradient model have been utilised for nanotubes. Furthermore, an analytical solution was presented by Setoodeh et al. [17] to predict the post-buckling response of CNTs via use of the Eringen theory of elasticity. Moreover, this nonlocal theory was used by Aydogdu [18] to analyse the longitudinal vibration of nanorods and CNTs embedded in a polymer matrix via a size-dependent model since size effects are important at small-scale levels [19]. Valipour et al. [20] studied the nonlinear vibration of nanotubes conveying fluid via a nonlocal model and a perturbation method. In another investigation, She et al. [21] explored the nonlinear static deflection and oscillation of porous small-scale tubes made of functionally graded materials. Khosravani and Weinberg [22] studied the mechanics of composite T-joint connections subject to various conditions. Malekzadeh and Shojaee [6] also examined the free vibration of nanobeams with a variable cross-sectional area by developing a nonlocal beam model incorporating the effects of large amplitudes since large deformations are important in many systems such as resonators [23] and actuators [24] as well as many structures such as small-scale beams [25] and plates [26]. The linear time-dependent deformation of nanoscale mass sensors using CNTs was studied by Aydogdu and Filiz [27] via a beam theory and the Eringen theory of elasticity. The influence of the internal friction on the oscillation of CNTs was

explored by Chang and Lee [28] within the framework of a nonlocal theoretical model. Furthermore, Lei et al. [29] suggested a viscoelastic model to describe the internal friction effect on the vibration of tubes at ultrasmall levels; they used the Kelvin–Voigt model. The vibration and buckling of viscoelastic CNTs containing fluid flow were investigated by Bahaadini and Hosseini [30] with the help of the Eringen theory of elasticity. Moreover, Zhang et al. [31] analysed the vibration of axially prestressed nanoscale beams with viscoelastic mechanical properties. The dynamics of viscoelastic nanocomposites made of CNTs with small deformations was also studied by Karlicic et al. [32] employing a nonlocal theoretical model; in their analysis, it was assumed that the nanocomposite was subject to a magnetic loading. Mohammadimehr et al. [33] used a size-dependent plate theory with consideration of shear deformations for examining the linear vibration of CNT-reinforced composite ultrasmall plates incorporating the internal energy loss; they employed a meshless technique in order to obtain the linear vibration characteristics.

More lately, a refined scale-dependent beam model based on a strain gradient model and the Eringen theory has been introduced [34]. It has been shown that the mechanical behaviour predicted using this theory is reasonably consistent with molecular dynamics (MD) results while neither the classical elasticity nor the nonlocal theory can estimate the mechanical behaviour properly [35]. The literature on the time-dependent deformation analysis of viscoelastic carbon nanotubes employing the nonlocal strain gradient theory (NSGT) is restricted. Few linear studies have been reported on the mechanical behaviour of viscoelastic CNTs using NSGT-based models [36, 37]. In addition, Ghayesh and Farajpour [38] developed a NSGT model for the large-amplitude oscillation of nanotubes; the effects of coupled motions and internal energy loss

were not captured in this investigation. Moreover, in another analysis reported in Ref. [39], the effects of a geometric imperfection on the nonlinear mechanics of nanotubes were investigated; the internal energy loss was not considered in this analysis. Ghayesh et al. [40] also utilised the couple stress theory so as to analyse chaos in microscale tubes conveying pulsatile microfluid; nonlocal and strain gradient effects were not incorporated. To the best of authors' knowledge, no investigation has been performed on the coupled dynamics of viscoelastic CNT via the NSGT yet. Recently, it has been reported that taking into account both longitudinal and transverse displacements (i.e. coupled dynamic analysis) at small-scale levels is of high significance in order to obtain more accurate results [41].

The aim of the present investigation is to comprehensively analyse scale effects on the nonlinear dynamic behaviour of viscoelastic CNTs incorporating both displacements along the longitudinal and transverse directions. Large deformations induced by the geometric nonlinearity are also incorporated into the scale-dependent formulation. Scale effects are captured via a nonlocal strain gradient model. The NSGT enable the continuum model to describe both the stiffness-hardening and –softening behaviours. Furthermore, the Kelvin–Voigt approach is employed to describe the influence of internal energy loss. According to the Euler–Bernoulli theory, the NSGT and the Hamilton principle, the nonlinear scale-dependent equations of motions are derived for both displacements along the longitudinal and transverse directions. In order to obtain an accurate numerical solution, the Galerkin scheme of discretisation and a continuation approach are utilised. The role of different nanosystem parameters in the nonlinear coupled dynamics of viscoelastic CNTs is examined.

2. A NSGT coupled viscoelastic tube model

A scale-dependent couple NSGT-based model is developed in the following so as to investigate the nonlinear dynamics of viscoelastic CNTs incorporating large deflections [42]. Both displacements along the longitudinal and transverse directions are taken into consideration. Figure 1 depicts a clamped-clamped CNT subject to an external loading along the transverse direction. The length and the average diameter of the CNT are indicated by *L* and *d*, respectively. The *x* axis of the coordinate frame is taken along the length of the nanotube while the *z* axis is taken along its thickness.

Using the model of Euler–Bernoulli beams, the nonlinear relation between the strain and displacement components is given by [43]

$$\varepsilon_{xx} = \frac{\partial u}{\partial x} + \frac{1}{2}\left(\frac{\partial w}{\partial x}\right)^2 - z\frac{\partial^2 w}{\partial x^2}, \tag{1}$$

where ε_{xx}, *u* and *w* are the axial strain, the axial displacement and the transverse displacement [44]. The NSGT stress of the CNT with consideration of the internal energy loss [45] can be written as [34]

$$t_{xx} - \left(e_0 a\right)^2 \nabla^2 t_{xx} = E\varepsilon_{xx} + \eta\frac{\partial \varepsilon_{xx}}{\partial t} - El_{sg}^2\nabla^2\varepsilon_{xx} - \eta l_{sg}^2\nabla^2\frac{\partial \varepsilon_{xx}}{\partial t}, \tag{2}$$

where t_{xx}, *E* and η denote the axial total stress, Young's modulus and the viscosity constant of the single-walled carbon nanotube, respectively; l_{sg} represents the strain gradient parameter while $e_0 a$ indicates the nonlocal parameter [46]; e_0 and *a* are respectively a constant for calibrating the continuum model and an internal characteristic length [47]; in Eq. (2), ∇^2 stands for the Laplace operator [48]. It is worth stating that the terms with $e_0 a$ are related to nonlocal

effects while the terms with l_{sg} incorporates strain gradient influences. Strain gradient and nonlocal parameters can be determined from the experimental or molecular dynamics results. The former is utilised to simulate the effects of large deformation gradients at small-scales while the latter is associated with a decrease in structure stiffness. The stress resultants are given by

$$\left\langle N_{xx}, M_{xx} \right\rangle = \int_A t_{xx} \left\langle 1, z \right\rangle dA, \tag{3}$$

in which A is the cross-sectional area [49]. N_{xx} and M_{xx} stand for the force and moment resultants. Substituting Eq. (1) into Eq. (2) and then using Eq. (3), one obtains

$$\begin{aligned}
&N_{xx} - \left(e_0 a\right)^2 \nabla^2 N_{xx} = EA\left(\frac{\partial u}{\partial x} + \frac{1}{2}\left(\frac{\partial w}{\partial x}\right)^2\right) + \eta A\left(\frac{\partial^2 u}{\partial t \partial x} + \frac{\partial w}{\partial x}\frac{\partial^2 w}{\partial t \partial x}\right) \\
&-EAl_{sg}^2 \nabla^2\left(\frac{\partial u}{\partial x} + \frac{1}{2}\left(\frac{\partial w}{\partial x}\right)^2\right) - \eta A l_{sg}^2 \nabla^2\left(\frac{\partial^2 u}{\partial t \partial x} + \frac{\partial w}{\partial x}\frac{\partial^2 w}{\partial t \partial x}\right), \\
&M_{xx} - \left(e_0 a\right)^2 \nabla^2 M_{xx} = -EI\frac{\partial^2 w}{\partial x^2} - \eta I \frac{\partial^3 w}{\partial t \partial x^2} \\
&+EIl_{sg}^2 \nabla^2 \frac{\partial^2 w}{\partial x^2} + \eta I l_{sg}^2 \nabla^2 \frac{\partial^3 w}{\partial t \partial x^2},
\end{aligned} \tag{4}$$

where I is the tube moment of inertia [50]. According to the NSGT, the variation of the CNT elastic energy (U_{el}) is expressed as

$$\begin{aligned}
&\delta U_{el} = \iiint_V \sigma_{xx(el)} \delta\varepsilon_{xx} dV + \iiint_V \sigma^{(1)}_{xx(el)} \nabla \delta\varepsilon_{xx} dV = \iiint_V \left[\sigma_{xx(el)} - \nabla \sigma^{(1)}_{xx(el)}\right] \delta\varepsilon_{xx} dV \\
&+\left[\iint_A \sigma^{(1)}_{xx(el)} \delta\varepsilon_{xx} dA\right]_0^L = \iiint_V t_{xx(el)} \delta\varepsilon_{xx} dV + \left[\iint_A \sigma^{(1)}_{xx(el)} \delta\varepsilon_{xx} dA\right]_0^L.
\end{aligned} \tag{5}$$

Here $\sigma_{xx(el)}$, $\sigma^{(1)}_{xx(el)}$, ∇ and V are the elastic part of the axial zeroth-order nonlocal stress, the elastic part of the axial first-order nonlocal stress, the gradient operator and the volume of the

CNT, respectively. In addition, the variation of the work carried out by the viscous parts of nonlocal stresses (W_{vis}) is given by

$$\delta W_{vis} = -\iiint_V \sigma_{xx(vis)} \delta\varepsilon_{xx} dV - \iiint_V \sigma^{(1)}_{xx(vis)} \nabla \delta\varepsilon_{xx} dV = -\iiint_V \left[\sigma_{xx(vis)} - \nabla \sigma^{(1)}_{xx(vis)} \right] \delta\varepsilon_{xx} dV$$
$$-\left[\iint_A \sigma^{(1)}_{xx(vis)} \delta\varepsilon_{xx} dA \right]_0^L = -\iiint_V t_{xx(vis)} \delta\varepsilon_{xx} dV - \left[\iint_A \sigma^{(1)}_{xx(vis)} \delta\varepsilon_{xx} dA \right]_0^L, \quad (6)$$

where $\sigma_{xx(vis)}$ and $\sigma^{(1)}_{xx(vis)}$ denote the viscoelastic parts of the axial zeroth- and first-order nonlocal stresses, respectively. The relations between the total, zeroth- and first-order nonlocal stresses are defined as

$$\begin{aligned} t_{xx} &= \sigma_{xx} - \nabla \sigma^{(1)}_{xx}, \\ t_{xx(el)} &= \sigma_{xx(el)} - \nabla \sigma^{(1)}_{xx(el)}, \\ t_{xx(vis)} &= \sigma_{xx(vis)} - \nabla \sigma^{(1)}_{xx(vis)}. \end{aligned} \quad (7)$$

On the other hand, the relations between the elastic and viscoelastic parts of nonlocal stresses are given by

$$\begin{aligned} t_{xx} &= t_{xx(el)} + t_{xx(vis)}, \\ \sigma_{xx} &= \sigma_{xx(el)} + \sigma_{xx(vis)}, \\ \sigma^{(1)}_{xx} &= \sigma^{(1)}_{xx(el)} + \sigma^{(1)}_{xx(vis)}. \end{aligned} \quad (8)$$

Now let us consider a viscoelastic single-walled CNT of mass per length m. One can formulate the variation of the total motion energy (T_k) as

$$\delta T_k = m \left(\int_0^L \frac{\partial u}{\partial t} \delta \frac{\partial u}{\partial t} dx + \int_0^L \frac{\partial w}{\partial t} \delta \frac{\partial w}{\partial t} dx \right). \quad (9)$$

The viscoelastic CNT is subject to an external load $f(x,t)$ in the z direction. The variation of the work done by this load (W_F) can be written as [51]

$$\delta W_F = \int_0^L f(x,t) \delta w \, \mathrm{d}x. \quad (10)$$

It is assumed that the variation of the external load is of the harmonic one. In this way, one can write [52]

$$f(x,t)=F\left(x\right)\cos\left(\omega t\right), \tag{11}$$

in which $F(x)$ and ω are the forcing amplitude and the excitation frequency of the external load, respectively. The variation of the elastic energy due to the elastic polymer matrix (U_{pm}) can be formulated as

$$\delta U_{pm}=k_1\int_0^L w\delta w\,\mathrm{d}x+k_2\int_0^L w^3\delta w\,\mathrm{d}x, \tag{12}$$

where k_1 and k_2 stand for the linear and nonlinear constants of the elastic polymer matrix, respectively. The Hamilton energy/work principle, as a derivation method, is given by

$$\int_{t_1}^{t_2}\left(\delta W_F+\delta T_k+\delta W_{vis}-\delta U_{el}-\delta U_{pm}\right)\mathrm{d}t=0. \tag{13}$$

Substituting Eq. (11) into Eq. (10) and then substituting the resultant equation as well as Eqs. (5), (6), (9) and (12) into Eq. (13), one can obtain

$$\begin{aligned}&\frac{1}{m}\frac{\partial N_{xx}}{\partial x}=\frac{\partial^2 u}{\partial t^2},\\&\frac{1}{m}\frac{\partial^2 M_{xx}}{\partial x^2}+\frac{1}{m}\frac{\partial}{\partial x}\left(N_{xx}\frac{\partial w}{\partial x}\right)+\frac{f}{m}-\frac{1}{m}\left(k_1w+k_2w^3\right)=\frac{\partial^2 w}{\partial t^2}.\end{aligned} \tag{14}$$

The following expressions can be derived for the force and moment stress resultants of the CNT via use of Eqs. (4) and (14)

$$\begin{aligned}N_{xx}=&EA\left(\frac{\partial u}{\partial x}+\frac{1}{2}\left(\frac{\partial w}{\partial x}\right)^2\right)+\eta A\left(\frac{\partial^2 u}{\partial t\partial x}+\frac{\partial w}{\partial x}\frac{\partial^2 w}{\partial t\partial x}\right)\\&-EAl_{sg}^2\nabla^2\left(\frac{\partial u}{\partial x}+\frac{1}{2}\left(\frac{\partial w}{\partial x}\right)^2\right)-\eta Al_{sg}^2\nabla^2\left(\frac{\partial^2 u}{\partial t\partial x}+\frac{\partial w}{\partial x}\frac{\partial^2 w}{\partial t\partial x}\right)+m\left(e_0a\right)^2\frac{\partial^3 u}{\partial x\partial t^2},\end{aligned}$$

$$M_{xx} = -EI\frac{\partial^2 w}{\partial x^2} - \eta I\frac{\partial^3 w}{\partial t\partial x^2} + EIl_{sg}^2\nabla^2\frac{\partial^2 w}{\partial x^2} + \eta Il_{sg}^2\nabla^2\frac{\partial^3 w}{\partial t\partial x^2}$$
$$+m\left(e_0 a\right)^2\frac{\partial^2 w}{\partial t^2} - \left(e_0 a\right)^2\frac{\partial}{\partial x}\left(N_{xx}\frac{\partial w}{\partial x}\right) - \left(e_0 a\right)^2\left[f - \left(k_1 w + k_2 w^3\right)\right]. \quad (15)$$

Inserting Eq. (15) into Eq. (14) leads to the following coupled nonlinear equations for viscoelastic CNTs subject to an external load with constant forcing amplitude (i.e. $F(x)=F_1$)

$$EA\left(\frac{\partial^2 u}{\partial x^2} + \frac{\partial w}{\partial x}\frac{\partial^2 w}{\partial x^2}\right) - EAl_{sg}^2\left(\frac{\partial^4 u}{\partial x^4} + 3\frac{\partial^2 w}{\partial x^2}\frac{\partial^3 w}{\partial x^3} + \frac{\partial w}{\partial x}\frac{\partial^4 w}{\partial x^4}\right)$$
$$+\eta A\left(\frac{\partial^3 u}{\partial t\partial x^2} + \frac{\partial^2 w}{\partial x^2}\frac{\partial^2 w}{\partial t\partial x} + \frac{\partial w}{\partial x}\frac{\partial^3 w}{\partial t\partial x^2}\right) - \eta Al_{sg}^2\left(\frac{\partial^5 u}{\partial t\partial x^4} + \frac{\partial^4 w}{\partial x^4}\frac{\partial^2 w}{\partial t\partial x}\right. \quad (16)$$
$$\left.+3\frac{\partial^3 w}{\partial x^3}\frac{\partial^3 w}{\partial t\partial x^2} + 3\frac{\partial^2 w}{\partial x^2}\frac{\partial^4 w}{\partial t\partial x^3} + \frac{\partial w}{\partial x}\frac{\partial^5 w}{\partial t\partial x^4}\right) = m\frac{\partial^2 u}{\partial t^2} - m\left(e_0 a\right)^2\frac{\partial^4 u}{\partial x^2\partial t^2},$$

$$-EI\left(\frac{\partial^4 w}{\partial x^4}-l_{sg}^2\frac{\partial^6 w}{\partial x^6}\right)-\eta I\left(\frac{\partial^5 w}{\partial t\partial x^4}-l_{sg}^2\frac{\partial^7 w}{\partial t\partial x^6}\right)+EA\left[\frac{\partial^2 w}{\partial x^2}-\left(e_0a\right)^2\frac{\partial^4 w}{\partial x^4}\right]\left[\frac{\partial u}{\partial x}+\frac{1}{2}\left(\frac{\partial w}{\partial x}\right)^2\right]$$

$$+EA\left[\frac{\partial w}{\partial x}-3\left(e_0a\right)^2\frac{\partial^3 w}{\partial x^3}\right]\left(\frac{\partial^2 u}{\partial x^2}+\frac{\partial w}{\partial x}\frac{\partial^2 w}{\partial x^2}\right)$$

$$-EA\left\{\left[l_{sg}^2+3\left(e_0a\right)^2\right]\frac{\partial^2 w}{\partial x^2}-\left(e_0a\right)^2 l_{sg}^2\frac{\partial^4 w}{\partial x^4}\right\}\left[\frac{\partial^3 u}{\partial x^3}+\left(\frac{\partial^2 w}{\partial x^2}\right)^2+\frac{\partial w}{\partial x}\frac{\partial^3 w}{\partial x^3}\right]$$

$$-EA\left\{\left[l_{sg}^2+\left(e_0a\right)^2\right]\frac{\partial w}{\partial x}-3\left(e_0a\right)^2 l_{sg}^2\frac{\partial^3 w}{\partial x^3}\right\}\left(\frac{\partial^4 u}{\partial x^4}+3\frac{\partial^2 w}{\partial x^2}\frac{\partial^3 w}{\partial x^3}+\frac{\partial w}{\partial x}\frac{\partial^4 w}{\partial x^4}\right)$$

$$+3EAl_{sg}^2\left(e_0a\right)^2\left(\frac{\partial^2 w}{\partial x^2}\right)\left[\frac{\partial^5 u}{\partial x^5}+3\left(\frac{\partial^3 w}{\partial x^3}\right)^2+4\frac{\partial^2 w}{\partial x^2}\frac{\partial^4 w}{\partial x^4}+\frac{\partial w}{\partial x}\frac{\partial^5 w}{\partial x^5}\right]$$

$$+EA\left(e_0a\right)^2 l_{sg}^2\frac{\partial w}{\partial x}\left(\frac{\partial^6 u}{\partial x^6}+10\frac{\partial^3 w}{\partial x^3}\frac{\partial^4 w}{\partial x^4}+5\frac{\partial^2 w}{\partial x^2}\frac{\partial^5 w}{\partial x^5}+\frac{\partial w}{\partial x}\frac{\partial^6 w}{\partial x^6}\right)$$

$$+\eta A\left[\frac{\partial^2 w}{\partial x^2}-\left(e_0a\right)^2\frac{\partial^4 w}{\partial x^4}\right]\left(\frac{\partial^2 u}{\partial t\partial x}+\frac{\partial w}{\partial x}\frac{\partial^2 w}{\partial t\partial x}\right)$$

$$+\eta A\left[\frac{\partial w}{\partial x}-3\left(e_0a\right)^2\frac{\partial^3 w}{\partial x^3}\right]\left(\frac{\partial^3 u}{\partial t\partial x^2}+\frac{\partial^2 w}{\partial x^2}\frac{\partial^2 w}{\partial t\partial x}+\frac{\partial w}{\partial x}\frac{\partial^3 w}{\partial t\partial x^2}\right)$$

$$-\eta A\left\{\left[l_{sg}^2+3\left(e_0a\right)^2\right]\frac{\partial^2 w}{\partial x^2}-\left(e_0a\right)^2 l_{sg}^2\frac{\partial^4 w}{\partial x^4}\right\}\times$$

$$\left(\frac{\partial^4 u}{\partial t\partial x^3}+\frac{\partial^3 w}{\partial x^3}\frac{\partial^2 w}{\partial t\partial x}+2\frac{\partial^2 w}{\partial x^2}\frac{\partial^3 w}{\partial t\partial x^2}+\frac{\partial w}{\partial x}\frac{\partial^4 w}{\partial t\partial x^3}\right)$$

$$
\begin{aligned}
&-\eta A\left\{\left[l_{sg}^2+\left(e_0a\right)^2\right]\frac{\partial w}{\partial x}-3\left(e_0a\right)^2 l_{sg}^2\frac{\partial^3 w}{\partial x^3}\right\}\left(\frac{\partial^5 u}{\partial t\partial x^4}+\frac{\partial^4 w}{\partial x^4}\frac{\partial^2 w}{\partial t\partial x}+3\frac{\partial^2 w}{\partial x^2}\frac{\partial^4 w}{\partial t\partial x^3}\right.\\
&\left.+3\frac{\partial^3 w}{\partial x^3}\frac{\partial^3 w}{\partial t\partial x^2}+\frac{\partial w}{\partial x}\frac{\partial^5 w}{\partial t\partial x^4}\right)+3\eta A\left(e_0a\right)^2 l_{sg}^2\frac{\partial^2 w}{\partial x^2}\times\\
&\left(\frac{\partial^6 u}{\partial t\partial x^5}+\frac{\partial^5 w}{\partial x^5}\frac{\partial^2 w}{\partial t\partial x}+4\frac{\partial^4 w}{\partial x^4}\frac{\partial^3 w}{\partial t\partial x^2}+6\frac{\partial^3 w}{\partial x^3}\frac{\partial^4 w}{\partial t\partial x^3}+4\frac{\partial^2 w}{\partial x^2}\frac{\partial^5 w}{\partial t\partial x^4}+\frac{\partial w}{\partial x}\frac{\partial^6 w}{\partial t\partial x^5}\right)\\
&+\eta A\left(e_0a\right)^2 l_{sg}^2\frac{\partial w}{\partial x}\left(\frac{\partial^7 u}{\partial t\partial x^6}+\frac{\partial^6 w}{\partial x^6}\frac{\partial^2 w}{\partial t\partial x}+5\frac{\partial^5 w}{\partial x^5}\frac{\partial^3 w}{\partial t\partial x^2}+10\frac{\partial^4 w}{\partial x^4}\frac{\partial^4 w}{\partial t\partial x^3}\right.\\
&\left.+10\frac{\partial^3 w}{\partial x^3}\frac{\partial^5 w}{\partial t\partial x^4}+5\frac{\partial^2 w}{\partial x^2}\frac{\partial^6 w}{\partial t\partial x^5}+\frac{\partial w}{\partial x}\frac{\partial^7 w}{\partial t\partial x^6}\right)\\
&+m\left(e_0a\right)^2\left[\frac{\partial^2 w}{\partial x^2}-\left(e_0a\right)^2\frac{\partial^4 w}{\partial x^4}\right]\frac{\partial^3 u}{\partial x\partial t^2}+m\left(e_0a\right)^2\left[\frac{\partial w}{\partial x}-3\left(e_0a\right)^2\frac{\partial^3 w}{\partial x^3}\right]\frac{\partial^4 u}{\partial x^2\partial t^2}\\
&-3m\left(e_0a\right)^4\frac{\partial^2 w}{\partial x^2}\frac{\partial^5 u}{\partial x^3\partial t^2}-m\left(e_0a\right)^4\frac{\partial w}{\partial x}\frac{\partial^6 u}{\partial x^4\partial t^2}\\
&-\left(k_1w+k_2w^3\right)+\left(e_0a\right)^2\left[k_1\frac{\partial^2 w}{\partial x^2}+6k_2w\left(\frac{\partial w}{\partial x}\right)^2+3k_2w^2\frac{\partial^2 w}{\partial x^2}\right]\\
&=-F_1\cos\left(\omega t\right)+m\left[\frac{\partial^2 w}{\partial t^2}-\left(e_0a\right)^2\frac{\partial^4 w}{\partial x^2\partial t^2}\right].
\end{aligned}
\tag{17}
$$

To obtain a numerical solution, first the coupled differential equations (i.e. Eqs. (16) and (17)) should be made non-dimensional using the following non-dimensional parameters

$$
\begin{aligned}
&x^*=\frac{x}{L},\ u^*=\frac{u}{r},\ w^*=\frac{w}{r},\ \chi_{nl}=\frac{e_0a}{L},\\
&\chi_{sg}=\frac{l_{sg}}{L},\ \eta^*=\sqrt{\frac{EI}{m}}\frac{\eta}{EL^2},\ K_1=\frac{k_1L^4}{EI},\ K_2=\frac{k_2L^4r^2}{EI},\\
&\beta=\frac{L}{r},\ r=\sqrt{\frac{I}{A}},\ F_1^*=\frac{F_1L^3}{EI},\ t^*=\frac{t}{L^2}\sqrt{\frac{EI}{m}},\ \Omega=\sqrt{\frac{L^4m}{EI}}\omega.
\end{aligned}
\tag{18}
$$

Here β is the slenderness ratio, and r denotes the gyration radius of the viscoelastic CNT. Employing the above non-dimensional parameters, Eqs. (16) and (17) can be rewritten as

$$\frac{\partial^2 u}{\partial t^2}-\chi_{nl}^2\frac{\partial^4 u}{\partial x^2\partial t^2}-\beta\left(\beta\frac{\partial^2 u}{\partial x^2}+\frac{\partial w}{\partial x}\frac{\partial^2 w}{\partial x^2}\right)+\beta\chi_{sg}^2\left(\beta\frac{\partial^4 u}{\partial x^4}+3\frac{\partial^2 w}{\partial x^2}\frac{\partial^3 w}{\partial x^3}+\frac{\partial w}{\partial x}\frac{\partial^4 w}{\partial x^4}\right)$$
$$-\beta\eta\left(\beta\frac{\partial^3 u}{\partial t\partial x^2}+\frac{\partial^2 w}{\partial x^2}\frac{\partial^2 w}{\partial t\partial x}+\frac{\partial w}{\partial x}\frac{\partial^3 w}{\partial t\partial x^2}\right)+\beta\eta\chi_{sg}^2\left(\beta\frac{\partial^5 u}{\partial t\partial x^4}+\frac{\partial^4 w}{\partial x^4}\frac{\partial^2 w}{\partial t\partial x}\right. \tag{19}$$
$$\left.+3\frac{\partial^3 w}{\partial x^3}\frac{\partial^3 w}{\partial t\partial x^2}+3\frac{\partial^2 w}{\partial x^2}\frac{\partial^4 w}{\partial t\partial x^3}+\frac{\partial w}{\partial x}\frac{\partial^5 w}{\partial t\partial x^4}\right)=0,$$

$$\frac{\partial^2 w}{\partial t^2}-\chi_{nl}^2\frac{\partial^4 w}{\partial x^2\partial t^2}-F_1\beta\cos(\Omega t)+\frac{\partial^4 w}{\partial x^4}-\chi_{sg}^2\frac{\partial^6 w}{\partial x^6}+\eta\left(\frac{\partial^5 w}{\partial t\partial x^4}-\chi_{sg}^2\frac{\partial^7 w}{\partial t\partial x^6}\right)$$
$$-\left(\frac{\partial^2 w}{\partial x^2}-\chi_{nl}^2\frac{\partial^4 w}{\partial x^4}\right)\left[\beta\frac{\partial u}{\partial x}+\frac{1}{2}\left(\frac{\partial w}{\partial x}\right)^2\right]-\left(\frac{\partial w}{\partial x}-3\chi_{nl}^2\frac{\partial^3 w}{\partial x^3}\right)\left(\beta\frac{\partial^2 u}{\partial x^2}+\frac{\partial w}{\partial x}\frac{\partial^2 w}{\partial x^2}\right)$$
$$+\left[\left(\chi_{sg}^2+3\chi_{nl}^2\right)\frac{\partial^2 w}{\partial x^2}-\chi_{nl}^2\chi_{sg}^2\frac{\partial^4 w}{\partial x^4}\right]\left[\beta\frac{\partial^3 u}{\partial x^3}+\left(\frac{\partial^2 w}{\partial x^2}\right)^2+\frac{\partial w}{\partial x}\frac{\partial^3 w}{\partial x^3}\right]$$
$$+\left[\left(\chi_{sg}^2+\chi_{nl}^2\right)\frac{\partial w}{\partial x}-3\chi_{nl}^2\chi_{sg}^2\frac{\partial^3 w}{\partial x^3}\right]\left(\beta\frac{\partial^4 u}{\partial x^4}+3\frac{\partial^2 w}{\partial x^2}\frac{\partial^3 w}{\partial x^3}+\frac{\partial w}{\partial x}\frac{\partial^4 w}{\partial x^4}\right)$$
$$-3\chi_{nl}^2\chi_{sg}^2\frac{\partial^2 w}{\partial x^2}\left[\beta\frac{\partial^5 u}{\partial x^5}+3\left(\frac{\partial^3 w}{\partial x^3}\right)^2+4\frac{\partial^2 w}{\partial x^2}\frac{\partial^4 w}{\partial x^4}+\frac{\partial w}{\partial x}\frac{\partial^5 w}{\partial x^5}\right]$$
$$-\chi_{nl}^2\chi_{sg}^2\frac{\partial w}{\partial x}\left[\beta\frac{\partial^6 u}{\partial x^6}+10\frac{\partial^3 w}{\partial x^3}\frac{\partial^4 w}{\partial x^4}+5\frac{\partial^2 w}{\partial x^2}\frac{\partial^5 w}{\partial x^5}+\frac{\partial w}{\partial x}\frac{\partial^6 w}{\partial x^6}\right]$$
$$-\eta\left(\frac{\partial^2 w}{\partial x^2}-\chi_{nl}^2\frac{\partial^4 w}{\partial x^4}\right)\left(\beta\frac{\partial^2 u}{\partial t\partial x}+\frac{\partial w}{\partial x}\frac{\partial^2 w}{\partial t\partial x}\right)$$
$$-\eta\left(\frac{\partial w}{\partial x}-3\chi_{nl}^2\frac{\partial^3 w}{\partial x^3}\right)\left(\beta\frac{\partial^3 u}{\partial t\partial x^2}+\frac{\partial^2 w}{\partial x^2}\frac{\partial^2 w}{\partial t\partial x}+\frac{\partial w}{\partial x}\frac{\partial^3 w}{\partial t\partial x^2}\right)$$
$$+\eta\left[\left(3\chi_{nl}^2+\chi_{sg}^2\right)\frac{\partial^2 w}{\partial x^2}-\chi_{nl}^2\chi_{sg}^2\frac{\partial^4 w}{\partial x^4}\right]\times$$
$$\left(\beta\frac{\partial^4 u}{\partial t\partial x^3}+\frac{\partial^3 w}{\partial x^3}\frac{\partial^2 w}{\partial t\partial x}+2\frac{\partial^2 w}{\partial x^2}\frac{\partial^3 w}{\partial t\partial x^2}+\frac{\partial w}{\partial x}\frac{\partial^4 w}{\partial t\partial x^3}\right)$$
$$+\eta\left[\left(\chi_{sg}^2+\chi_{nl}^2\right)\frac{\partial w}{\partial x}-3\chi_{nl}^2\chi_{sg}^2\frac{\partial^3 w}{\partial x^3}\right]\left(\beta\frac{\partial^5 u}{\partial t\partial x^4}+\frac{\partial^4 w}{\partial x^4}\frac{\partial^2 w}{\partial t\partial x}+3\frac{\partial^2 w}{\partial x^2}\frac{\partial^4 w}{\partial t\partial x^3}\right.$$
$$\left.+3\frac{\partial^3 w}{\partial x^3}\frac{\partial^3 w}{\partial t\partial x^2}+\frac{\partial w}{\partial x}\frac{\partial^5 w}{\partial t\partial x^4}\right)-3\eta\chi_{nl}^2\chi_{sg}^2\frac{\partial^2 w}{\partial x^2}\times$$
$$\left(\beta\frac{\partial^6 u}{\partial t\partial x^5}+\frac{\partial^5 w}{\partial x^5}\frac{\partial^2 w}{\partial t\partial x}+4\frac{\partial^4 w}{\partial x^4}\frac{\partial^3 w}{\partial t\partial x^2}+6\frac{\partial^3 w}{\partial x^3}\frac{\partial^4 w}{\partial t\partial x^3}+4\frac{\partial^2 w}{\partial x^2}\frac{\partial^5 w}{\partial t\partial x^4}+\frac{\partial w}{\partial x}\frac{\partial^6 w}{\partial t\partial x^5}\right)$$

$$
\begin{aligned}
&-\eta\chi_{nl}^2\chi_{sg}^2\frac{\partial w}{\partial x}\left(\beta\frac{\partial^7 u}{\partial t\partial x^6}+\frac{\partial^6 w}{\partial x^6}\frac{\partial^2 w}{\partial t\partial x}+5\frac{\partial^5 w}{\partial x^5}\frac{\partial^3 w}{\partial t\partial x^2}+10\frac{\partial^4 w}{\partial x^4}\frac{\partial^4 w}{\partial t\partial x^3}\right.\\
&\left.+10\frac{\partial^3 w}{\partial x^3}\frac{\partial^5 w}{\partial t\partial x^4}+5\frac{\partial^2 w}{\partial x^2}\frac{\partial^6 w}{\partial t\partial x^5}+\frac{\partial w}{\partial x}\frac{\partial^7 w}{\partial t\partial x^6}\right)\\
&-\frac{\chi_{nl}^2}{\beta}\left(\frac{\partial^2 w}{\partial x^2}-\chi_{nl}^2\frac{\partial^4 w}{\partial x^4}\right)\frac{\partial^3 u}{\partial x\partial t^2}-\frac{\chi_{nl}^2}{\beta}\left(\frac{\partial w}{\partial x}-3\chi_{nl}^2\frac{\partial^3 w}{\partial x^3}\right)\frac{\partial^4 u}{\partial x^2\partial t^2}\\
&+\frac{3\chi_{nl}^4}{\beta}\frac{\partial^2 w}{\partial x^2}\frac{\partial^5 u}{\partial x^3\partial t^2}+\frac{\chi_{nl}^4}{\beta}\frac{\partial w}{\partial x}\frac{\partial^6 u}{\partial x^4\partial t^2}+\left(K_1 w+K_2 w^3\right)\\
&-\chi_{nl}^2\left[K_1\frac{\partial^2 w}{\partial x^2}+6K_2 w\left(\frac{\partial w}{\partial x}\right)^2+3K_2 w^2\frac{\partial^2 w}{\partial x^2}\right]=0.
\end{aligned}
\tag{20}
$$

For the sake of convenience, the star notation is removed from the above equations. Assume that $r_i(t)$ and $\hat{u}_i(x)$ are respectively the axial generalised coordinate and shape function; also $q_i(t)$ and $\hat{w}_i(x)$ are employed to denote the transverse generalised coordinate and shape function, respectively. The displacement components can be described as

$$
\begin{aligned}
&u(x,t)=\sum_{i=1}^{N_x} r_i(t)\hat{u}_i(x),\\
&w(x,t)=\sum_{i=1}^{N_z} q_i(t)\hat{w}_i(x).
\end{aligned}
\tag{21}
$$

In the above relations, N_x and N_z represent the number of shape functions in the x and z directions, respectively [53]. Using Eqs. (21) in conjunction with the Galerkin scheme, one can discretise the coupled equations of motion as

$$\sum_{i=1}^{N_x}\ddot{r}_i\left(\int_0^1\hat{u}_i\hat{u}_k dx\right)-\chi_{nl}^2\sum_{i=1}^{N_x}\ddot{r}_i\left(\int_0^1\hat{u}_i''\hat{u}_k dx\right)-\beta\left[\beta\sum_{i=1}^{N_x}r_i\left(\int_0^1\hat{u}_i''\hat{u}_k dx\right)+\sum_{i=1}^{N_z}\sum_{j=1}^{N_z}q_jq_i\left(\int_0^1\hat{w}_i'\hat{w}_j''\hat{u}_k dx\right)\right]$$

$$+\beta\chi_{sg}^2\left[\beta\sum_{i=1}^{N_x}r_i\left(\int_0^1\hat{u}_i''''\hat{u}_k dx\right)+3\sum_{i=1}^{N_z}\sum_{j=1}^{N_z}q_jq_i\left(\int_0^1\hat{w}_i''\hat{w}_j'''\hat{u}_k dx\right)+\sum_{i=1}^{N_z}\sum_{j=1}^{N_z}q_jq_i\left(\int_0^1\hat{w}_i'\hat{w}_j''''\hat{u}_k dx\right)\right]$$

$$-\beta\eta\left[\beta\sum_{i=1}^{N_x}\dot{r}_i\left(\int_0^1\hat{u}_i''\hat{u}_k dx\right)+\sum_{i=1}^{N_z}\sum_{j=1}^{N_z}\dot{q}_jq_i\left(\int_0^1\hat{w}_i''\hat{w}_j'\hat{u}_k dx\right)+\sum_{i=1}^{N_z}\sum_{j=1}^{N_z}\dot{q}_jq_i\left(\int_0^1\hat{w}_i'\hat{w}_j''\hat{u}_k dx\right)\right]$$

$$+\beta\eta\chi_{sg}^2\left[\beta\sum_{i=1}^{N_x}\dot{r}_i\left(\int_0^1\hat{u}_i''''\hat{u}_k dx\right)+\sum_{i=1}^{N_z}\sum_{j=1}^{N_z}\dot{q}_jq_i\left(\int_0^1\hat{w}_i''''\hat{w}_j'\hat{u}_k dx\right)\right.$$

$$\left.+3\sum_{i=1}^{N_z}\sum_{j=1}^{N_z}\dot{q}_jq_i\left(\int_0^1\hat{w}_i'''\hat{w}_j''\hat{u}_k dx\right)+3\sum_{i=1}^{N_z}\sum_{j=1}^{N_z}\dot{q}_jq_i\left(\int_0^1\hat{w}_i''\hat{w}_j'''\hat{u}_k dx\right)+\sum_{i=1}^{N_z}\sum_{j=1}^{N_z}\dot{q}_jq_i\left(\int_0^1\hat{w}_i'\hat{w}_j''''\hat{u}_k dx\right)\right]=0, \qquad (22)$$

$$\sum_{i=1}^{N_z}\ddot{q}_i\left[\int_0^1\hat{w}_k\left(\hat{w}_i-\chi_{nl}^2\hat{w}_i''\right)dx\right]+\eta\sum_{i=1}^{N_z}\dot{q}_i\left[\int_0^1\hat{w}_k\left(\hat{w}''''-\chi_{sg}^2\hat{w}_i^{(6)}\right)dx\right]$$

$$+\sum_{i=1}^{N_z}q_i\left[\int_0^1\hat{w}_k\left(\hat{w}_i''''-\chi_{sg}^2\hat{w}_i^{(6)}\right)dx\right]-F_1\beta\left(\int_0^1\hat{w}_k dx\right)\cos(\Omega t)$$

$$-\int_0^1\left\{\sum_{i=1}^{N_z}q_i\hat{w}_k\left(\hat{w}_i''-\chi_{nl}^2\hat{w}_i''''\right)\left[\beta\sum_{i=1}^{N_x}r_i\hat{u}_i'+\frac{1}{2}\sum_{i=1}^{N_z}\sum_{j=1}^{N_z}q_jq_i\hat{w}_i'\hat{w}_j'\right]dx\right\}$$

$$-\int_0^1\left\{\left[\sum_{i=1}^{N_z}q_i\hat{w}_k\left(\hat{w}_i'-3\chi_{nl}^2\hat{w}_i'''\right)\right]\left(\beta\sum_{i=1}^{N_x}r_i\hat{u}_i''+\sum_{i=1}^{N_z}\sum_{j=1}^{N_z}q_jq_i\hat{w}_i'\hat{w}_j''\right)dx\right\}$$

$$+\int_0^1\left\{\left(\sum_{i=1}^{N_z}q_i\left[\left(\chi_{sg}^2+3\chi_{nl}^2\right)\hat{w}_i''-\chi_{nl}^2\chi_{sg}^2\hat{w}_i''''\right]\right)\left[\beta\sum_{i=1}^{N_x}r_i\hat{u}_i'''+\sum_{i=1}^{N_z}\sum_{j=1}^{N_z}q_jq_i\left(\hat{w}_i''\hat{w}_j''+\hat{w}_i'\hat{w}_j'''\right)\right]dx\right\}$$

$$+\int_0^1\left\{\left(\sum_{i=1}^{N_z}q_i\left[\left(\chi_{sg}^2+\chi_{nl}^2\right)\hat{w}_i'-3\chi_{nl}^2\chi_{sg}^2\hat{w}_i'''\right]\right)\left[\beta\sum_{i=1}^{N_x}r_i\hat{u}_i''''+\sum_{i=1}^{N_z}\sum_{j=1}^{N_z}q_jq_i\left(3\hat{w}_i''\hat{w}_j'''+\hat{w}_i'\hat{w}_j''''\right)\right]dx\right\}$$

$$-3\chi_{nl}^2\chi_{sg}^2\int_0^1\left\{\left(\sum_{i=1}^{N_z}q_i\hat{w}_k\hat{w}_i''\right)\left[\beta\sum_{i=1}^{N_x}r_i\hat{u}_i^{(5)}+\sum_{i=1}^{N_z}\sum_{j=1}^{N_z}q_jq_i\left(3\hat{w}_i'''\hat{w}_j'''+4\hat{w}_i''\hat{w}_j''''+\hat{w}_i'\hat{w}_j^{(5)}\right)\right]dx\right\}$$

$$-\chi_{nl}^2\chi_{sg}^2\int_0^1\left\{\left(\sum_{i=1}^{N_z}q_i\hat{w}_k\hat{w}_i'\right)\left[\beta\sum_{i=1}^{N_x}r_i\hat{u}_i^{(6)}+\sum_{i=1}^{N_z}\sum_{j=1}^{N_z}q_jq_i\left(10\hat{w}_i'''\hat{w}_j''''+5\hat{w}_i''\hat{w}_j^{(5)}+\hat{w}_i'\hat{w}_j^{(6)}\right)\right]dx\right\}$$

$$-\eta\int_0^1\left\{\left[\sum_{i=1}^{N_z}q_i\hat{w}_k\left(\hat{w}_i''-\chi_{nl}^2\hat{w}_i''''\right)\right]\left(\beta\sum_{i=1}^{N_x}\dot{r}_i\hat{u}_i'+\sum_{i=1}^{N_z}\sum_{j=1}^{N_z}\dot{q}_jq_i\hat{w}_i'\hat{w}_j'\right)dx\right\}$$

$$-\eta\int_0^1\left\{\left[\sum_{i=1}^{N_z}\sum_{i=1}^{N_z}q_i\hat{w}_k\left(\hat{w}_i'-3\chi_{nl}^2\hat{w}_i'''\right)\right]\left[\beta\sum_{i=1}^{N_x}\dot{r}_i\hat{u}_i''+\sum_{i=1}^{N_z}\sum_{j=1}^{N_z}\dot{q}_jq_i\left(\hat{w}_i''\hat{w}_j'+\hat{w}_i'\hat{w}_j''\right)\right]dx\right\}$$

$$+\eta\int_0^1\left\{\left(\sum_{i=1}^{N_z}q_i\hat{w}_k\left[\left(3\chi_{nl}^2+\chi_{sg}^2\right)\hat{w}_i''-\chi_{nl}^2\chi_{sg}^2\hat{w}_i''''\right]\right)\times\right.$$

$$\left.\left[\beta\sum_{i=1}^{N_x}\dot{r}_i\hat{u}_i'''+\sum_{i=1}^{N_z}\sum_{j=1}^{N_z}\dot{q}_jq_i\left(\hat{w}_i'''\hat{w}_j'+2\hat{w}_i''\hat{w}_j''+\hat{w}_i'\hat{w}_j'''\right)\right]dx\right\}$$

$$+\eta\int_0^1\left\{\left(\sum_{i=1}^{N_z}q_i\hat{w}_k\left[\left(\chi_{sg}^2+\chi_{nl}^2\right)\hat{w}_i'-3\chi_{nl}^2\chi_{sg}^2\hat{w}_i'''\right]\right)\times\right.$$

$$\left.\left[\beta\sum_{i=1}^{N_x}\dot{r}_i\hat{u}_i''''+\sum_{i=1}^{N_z}\sum_{j=1}^{N_z}\dot{q}_jq_i\left(\hat{w}_i''''\hat{w}_j'+3\hat{w}_i''\hat{w}_j'''+3\hat{w}_i'''\hat{w}_j''+\hat{w}_i'\hat{w}_j''''\right)\right]dx\right\}$$

$$-3\eta\chi_{nl}^2\chi_{sg}^2\int_0^1\left\{\left(\sum_{i=1}^{N_z}q_i\hat{w}_k\hat{w}_i''\right)\left[\beta\sum_{i=1}^{N_x}\dot{r}_i\hat{u}_i^{(5)}+\sum_{i=1}^{N_z}\sum_{j=1}^{N_z}\dot{q}_jq_i\left(\hat{w}_i^{(5)}\hat{w}_j'+4\hat{w}_i''''\hat{w}_j''\right.\right.\right.$$

$$\left.\left.\left.+6\hat{w}_i'''\hat{w}_j'''+4\hat{w}_i''\hat{w}_j''''+\hat{w}_i'\hat{w}_j^{(5)}\right)\right]dx\right\}-\eta\chi_{nl}^2\chi_{sg}^2\int_0^1\left\{\left(\sum_{i=1}^{N_z}q_i\hat{w}_k\hat{w}_i'\right)\left[\beta\sum_{i=1}^{N_x}\dot{r}_i\hat{u}_i^{(6)}+\right.\right.$$

$$\left.\left.\sum_{i=1}^{N_z}\sum_{j=1}^{N_z}\dot{q}_jq_i\left(\hat{w}_i^{(6)}\hat{w}_j'+5\hat{w}_i^{(5)}\hat{w}_j''+10\hat{w}_i''''\hat{w}_j'''+10\hat{w}_i'''\hat{w}_j''''+5\hat{w}_i''\hat{w}_j^{(5)}+\hat{w}_i'\hat{w}_j^{(6)}\right)\right]dx\right\}$$

$$-\frac{\chi_{nl}^2}{\beta}\int_0^1\left\{\left[\left(\sum_{i=1}^{N_x}\ddot{r}_i\hat{w}_k\hat{u}_i'\right)\left(\sum_{i=1}^{N_z}q_i\left(\hat{w}_i''-\chi_{nl}^2\hat{w}_i''''\right)\right)+\left(\sum_{i=1}^{N_x}\ddot{r}_i\hat{w}_k\hat{u}_i''\right)\left(\sum_{i=1}^{N_z}q_i\left(\hat{w}_i'-3\chi_{nl}^2\hat{w}_i'''\right)\right)\right]dx\right\}$$

$$+\frac{\chi_{nl}^4}{\beta}\sum_{i=1}^{N_z}\sum_{j=1}^{N_x}\ddot{r}_jq_i\left[\int_0^1\hat{w}_k\left(3\hat{w}_i''\hat{u}_j'''+\hat{w}_i'\hat{u}_j''''\right)dx\right]+K_1\sum_{i=1}^{N_z}q_i\left(\int_0^1\hat{w}_k\hat{w}_i dx\right)$$

$$+K_2\sum_{i=1}^{N_z}\sum_{j=1}^{N_z}\sum_{l=1}^{N_z}q_lq_jq_i\left(\int_0^1\hat{w}_k\hat{w}_i\hat{w}_j\hat{w}_l dx\right)-\chi_{nl}^2K_1\sum_{i=1}^{N_z}q_i\left(\int_0^1\hat{w}_k\hat{w}_i''dx\right)$$

$$-3\chi_{nl}^2K_2\sum_{l=1}^{N_z}\sum_{i=1}^{N_z}\sum_{j=1}^{N_z}q_iq_lq_j\left[\int_0^1\hat{w}_k\hat{w}_l\left(2\hat{w}_i'\hat{w}_j'+\hat{w}_j\hat{w}_i''\right)dx\right]=0. \tag{23}$$

To obtain the coupled dynamic characteristics of the viscoelastic CNT with clamped boundary conditions at both ends (see Fig. 1), a continuation solution method is used for a nanosystem with eight base functions along both directions. A computer program is written based on this solution method, which can be used for extracting unstable and stable branches as well as bifurcation points. At the first step, a continuation parameter such as the arclength *s* in the direction of a solution branch is employed. Then, a number of state variables are utilised for rewriting time-dependent differential equations. At the next step, to determine the equilibrium position, generalised coordinates are differentiated with respect to *s,* and Newton-Raphson technique is also utilised.

3. Numerical results

In this section, a chiral single-walled CNT with chirality (10,5) is taken into consideration to examine the coupled nonlinear dynamics. The length, thickness and average diameter of the CNT are set to 20, 0.34 and 1.0357 nm, respectively. The slenderness ratio, the strain gradient coefficient and the nonlocal coefficient are also as 51.8939, 0.05 and 0.1, respectively. The system elastic properties are assumed as E=1.0 TPa, ν=0.19, and ρ=2300 kg/m^3 in which E, ν and ρ represent the elasticity modulus, Poisson's ratio and the mass per unit volume of the chiral CNT. The viscosity coefficient of the nonlinear viscoelastic model is η=0.0005 while the modal damping ratio of the linear damping model is set to ζ=0.006.

Figure 2 demonstrates the frequency-amplitude diagrams of CNTs for the coupled nonlinear motion along both directions for χ_{nl} =0.1 and χ_{sg}=0.05. The forcing amplitude, the linear and nonlinear elastic constants of the foundation are taken as F_1=0.30, K_1=20.0 and K_2=25.0, respectively. The nonlinear coupled dynamics of viscoelastic CNTs embedded in an elastic medium is of hardening type. In fact, as the excitation frequency increases, first there is a gradual increase in motion amplitudes; however, it is followed by a sudden reduction in the motion amplitudes of the nanotube at the first saddle node. This sudden reduction can be interpreted as an increase in the stiffness (hardening behaviour). Two saddle nodes (SNs) are also found in the nonlinear dynamic behaviour of the nanosystem (SN$_1$: Ω/ω_1=1.2270; SN$_2$: Ω/ω_1=1.0465). Figure 3 shows the large-amplitude coupled dynamic characteristics of the viscoelastic CNT of Fig. 2 at Ω/ω_1=1.20; the time traces of q_1 and r_2 as well as their phase-plane diagrams are plotted.

Figure 4 indicates the influences of the nonlocality and strain gradients on the coupled frequency-amplitude response of the viscoelastic nanotube for the motions along both axes. The results of the nonlocal strain gradient model (χ_{nl} =0.1; χ_{sg}=0.05) are compared with those of the classical elasticity (χ_{nl} =0; χ_{sg}=0). The forcing amplitude, the linear and nonlinear constants of the elastic medium are assumed as F_1=0.30, K_1=20.0 and K_2=25.0, respectively. Moreover, the viscosity coefficient of the nonlinear viscoelastic model is η=0.0005. It is found that the NSGT resonance frequency is smaller than the classical one since nonlocal effects are dominant (the nonlocal coefficient is twice the strain gradient one), which yield a slight decrease in structure stiffness. In addition, the classical elasticity overestimates the peak amplitude of viscoelastic CNTs.

Plotted in Fig. 5 is the force-amplitude diagrams of the viscoelastic chiral CNT for χ_{nl} =0.1, χ_{sg}=0.05, F_1=0.30, K_1=20.0, K_2=25.0, and η=0.0005. Both stable and unstable responses are shown in the figure. It is observed that increasing the forcing amplitude leads to a gradual increase in the amount of the amplitude along both axes. However, this gradual increase is followed by a notable sudden increase at the first saddle node (F_1=0.6215). Another saddle node at F_1=0.1249 is also observed in the nonlinear coupled force-amplitude response of the viscoelastic CNT.

Figure 6 depicts the strain gradient and nonlocal effects on the force-amplitude diagrams of the viscoelastic CNT for the coupled motion. The non-dimensional parameters are set to K_1=20.0, K_2=25.0, η=0.0005, and Ω=24.0. Neglecting the NSGT effect results in lower forcing amplitudes associated with the saddle nodes. Furthermore, for large values of F_1, the classical

elasticity predicts smaller motion amplitudes than those of the NSGT while the classical elasticity overestimates the CNT amplitude for small forcing amplitudes.

Two damping mechanisms (i.e. the linear viscous damping and the Kelvin-Voigt nonlinear damping) are compared in Fig. 7. The nonlinear resonance frequency of the viscoelastic chiral CNT versus the forcing amplitude is plotted in this figure. It is found that the gap between the two damping mechanisms can be neglected for small forcing amplitudes. Nonetheless, for higher values of F_1, the linear damping mechanism leads to higher nonlinear resonance frequencies.

Illustrated in Fig. 8 is the nonlinear resonance amplitudes versus the forcing amplitude obtained based on two damping mechanisms. Again, it is observed that the difference between the two mechanisms can be neglected for small forcing amplitudes while for large ones, the Kelvin-Voigt nonlinear damping mechanism leads to smaller nonlinear resonance amplitudes along both axes.

The influence of the linear spring constant on the frequency-amplitude response of the viscoelastic chiral CNT for the coupled motion is shown in Fig. 9; the non-dimensional parameters are set to F_1=0.30, K_2=25.0, and η=0.0005. From the figure, it can be seen that higher linear spring constants result in higher non-dimensional excitation frequencies associated with the resonance. The mechanics reason for this is that increasing the linear spring constant increases the structure stiffness, especially at small-scale levels, and this consequently increases the resonance frequency of nanotubes. However, the peak amplitude is slightly smaller for higher linear spring constants.

Figure 10 demonstrates the influence of the linear spring stiffness on the force-amplitude response of the viscoelastic CNT for K_2=25.0, η=0.0005, and Ω=23.0. It can be concluded that the linear spring stiffness does not change the type and number of saddle nodes of the nanosystem. Nonetheless, increasing linear spring stiffness reduces the value of the forcing amplitude associated with saddle nodes.

4. Concluding remarks

The coupled mechanical behaviour of viscoelastic CNTs was studied taking into account both displacements along the longitudinal and transverse directions. The effects of large deformations induced by the geometric nonlinearity were also taken into account. The NSGT was used to capture scale effects on the coupled mechanical behaviour. In addition, the Kelvin–Voigt approach was employed for incorporating the influence of the internal energy loss. Applying the NSGT and the Hamilton principle, the scale-dependent equations of the coupled motion were derived for both displacements along the longitudinal and transverse directions. The Galerkin scheme of discretisation and a continuation approach were employed to obtain an accurate numerical solution.

From the numerical results, it was found that for higher values of the forcing amplitude, the linear damping mechanism results in overestimated nonlinear resonance frequencies. Moreover, the linear spring stiffness does not change the type and number of saddle nodes of the viscoelastic CNT. Nonetheless, higher linear spring constants lead to higher excitation frequencies associated with the resonance while the peak amplitude is slightly lower for higher spring stiffnesses. The coupled mechanics of viscoelastic CNTs embedded in an elastic bed is of

hardening type with two saddle nodes. Furthermore, it was concluded that the classical elasticity overestimates the peak amplitude of the nanosystem. The present nonlinear formulation and numerical results provide a theoretical platform for future experimental investigations on the nonlinear dynamics of nanotubes.

Appendix A. Comparison studies

A comparison with the existing results for the linear vibration of nanoscale tubes with simply supported ends [54] is given in Fig. 11 so as to validate the present formulation. The nonlocal and strain gradient parameters are $\chi_{nl} = e_0 a / L = 0.02$ and $\chi_{sg} = l_{sg} / L = 0.03$, respectively. Other nanosystem properties can be found in Refs. [54, 55]. The effects of the internal energy loss are ignored. Furthermore, the large deflections associated with the geometrical nonlinearity are not taken into consideration. From the figure, a good match between the results of the present formulation and those extracted by Li et al. [54] using the NSGT is found.

A comparison between different theories involving the classical, nonlocal, strain gradient and nonlocal strain gradient is given in Fig. 12 for the natural frequencies of simply supported nanoscale tubes. The classical, nonlocal, strain gradient and nonlocal strain gradient theories are denoted by CT, NT, ST and NSGT, respectively. Nanosystem properties are found in Refs. [54, 55]. The effects of the internal energy loss and large deformations are ignored. It can be seen that the NT gives the lowest natural frequency while the ST leads to the highest one. This

is rooted in the fact that strain gradient effects lead to an increase in structure stiffness whereas nonlocal effects yield a decrease in the stiffness.

References

[1] Suhr J, Koratkar N, Keblinski P, Ajayan P. Viscoelasticity in carbon nanotube composites. Nature materials. 2005;4(2):134.
[2] Setoodeh A, Malekzadeh P, Vosoughi A. Nonlinear free vibration of orthotropic graphene sheets using nonlocal Mindlin plate theory. Proceedings of the Institution of Mechanical Engineers, Part C: Journal of Mechanical Engineering Science. 2012;226(7):1896-906.
[3] Beni AA, Malekzadeh P. Nonlocal free vibration of orthotropic non-prismatic skew nanoplates. Composite Structures. 2012;94(11):3215-22.
[4] Malekzadeh P, Mohebpour S, Heydarpour Y. Nonlocal effect on the free vibration of short nanotubes embedded in an elastic medium. Acta Mechanica. 2012;223(6):1341-50.
[5] Malekzadeh P, Haghighi MG, Shojaee M. Nonlinear free vibration of skew nanoplates with surface and small scale effects. Thin-Walled Structures. 2014;78:48-56.
[6] Malekzadeh P, Shojaee M. Free vibration of nanoplates based on a nonlocal two-variable refined plate theory. Composite Structures. 2013;95:443-52.
[7] Asemi SR, Farajpour A. Vibration characteristics of double-piezoelectric-nanoplate-systems. IET Micro & Nano Letters. 2014;9(4):280-5.
[8] Aydogdu M, Elishakoff I. On the vibration of nanorods restrained by a linear spring in-span. Mechanics Research Communications. 2014;57:90-6.
[9] Iijima S. Helical microtubules of graphitic carbon. nature. 1991;354(6348):56.
[10] Kamali M, Shamsi M, Saidi A. Postbuckling of magneto-electro-elastic CNT-MT composite nanotubes resting on a nonlinear elastic medium in a non-uniform thermal environment. The European Physical Journal Plus. 2018;133(3):110.
[11] Ebrahimi F, Barati MR, Haghi P. Nonlocal thermo-elastic wave propagation in temperature-dependent embedded small-scaled nonhomogeneous beams. The European Physical Journal Plus. 2016;131(11):383.
[12] Hadi A, Nejad MZ, Hosseini M. Vibrations of three-dimensionally graded nanobeams. International Journal of Engineering Science. 2018;128:12-23.
[13] Omidian R, Beni YT, Mehralian F. Analysis of size-dependent smart flexoelectric nanobeams. The European Physical Journal Plus. 2017;132(11):481.
[14] Adeli MM, Hadi A, Hosseini M, Gorgani HH. Torsional vibration of nano-cone based on nonlocal strain gradient elasticity theory. The European Physical Journal Plus. 2017;132(9):393.
[15] Oskouie MF, Ansari R, Rouhi H. Stress-driven nonlocal and strain gradient formulations of Timoshenko nanobeams. The European Physical Journal Plus. 2018;133(8):336.
[16] Farajpour M, Shahidi A, Tabataba'i-Nasab F, Farajpour A. Vibration of initially stressed carbon nanotubes under magneto-thermal environment for nanoparticle delivery via higher-order nonlocal strain gradient theory. The European Physical Journal Plus. 2018;133(6):219.
[17] Setoodeh A, Khosrownejad M, Malekzadeh P. Exact nonlocal solution for postbuckling of single-walled carbon nanotubes. Physica E: Low-dimensional Systems and Nanostructures. 2011;43(9):1730-7.

[18] Aydogdu M. Longitudinal wave propagation in nanorods using a general nonlocal unimodal rod theory and calibration of nonlocal parameter with lattice dynamics. International Journal of Engineering Science. 2012;56:17-28.
[19] Ghayesh MH, Farokhi H, Alici G. Size-dependent performance of microgyroscopes. International Journal of Engineering Science. 2016;100:99-111.
[20] Valipour P, Ghasemi S, Khosravani MR, Ganji D. Theoretical analysis on nonlinear vibration of fluid flow in single-walled carbon nanotube. Journal of Theoretical and Applied Physics. 2016;10(3):211-8.
[21] She G-L, Yuan F-G, Ren Y-R, Liu H-B, Xiao W-S. Nonlinear bending and vibration analysis of functionally graded porous tubes via a nonlocal strain gradient theory. Composite Structures. 2018;203:614-23.
[22] Khosravani MR, Weinberg K. Characterization of sandwich composite T-joints under different ageing conditions. Composite Structures. 2018;197:80-8.
[23] Ghayesh MH, Farokhi H, Amabili M. Nonlinear behaviour of electrically actuated MEMS resonators. International Journal of Engineering Science. 2013;71:137-55.
[24] Farokhi H, Ghayesh MH. Nonlinear mechanics of electrically actuated microplates. International Journal of Engineering Science. 2018;123:197-213.
[25] Ghayesh MH, Amabili M, Farokhi H. Nonlinear forced vibrations of a microbeam based on the strain gradient elasticity theory. International Journal of Engineering Science. 2013;63:52-60.
[26] Gholipour A, Farokhi H, Ghayesh MH. In-plane and out-of-plane nonlinear size-dependent dynamics of microplates. Nonlinear Dynamics. 2015;79(3):1771-85.
[27] Aydogdu M, Filiz S. Modeling carbon nanotube-based mass sensors using axial vibration and nonlocal elasticity. Physica E: Low-dimensional Systems and Nanostructures. 2011;43(6):1229-34.
[28] Shu C. Differential quadrature and its application in engineering: Springer Science & Business Media; 2012.
[29] Lei Y, Adhikari S, Friswell M. Vibration of nonlocal Kelvin–Voigt viscoelastic damped Timoshenko beams. International Journal of Engineering Science. 2013;66:1-13.
[30] Bahaadini R, Hosseini M. Effects of nonlocal elasticity and slip condition on vibration and stability analysis of viscoelastic cantilever carbon nanotubes conveying fluid. Computational Materials Science. 2016;114:151-9.
[31] Zhang Y, Pang M, Fan L. Analyses of transverse vibrations of axially pretensioned viscoelastic nanobeams with small size and surface effects. Physics Letters A. 2016;380(29-30):2294-9.
[32] Karličić D, Murmu T, Cajić M, Kozić P, Adhikari S. Dynamics of multiple viscoelastic carbon nanotube based nanocomposites with axial magnetic field. Journal of Applied Physics. 2014;115(23):234303.
[33] Mohammadimehr M, Navi BR, Arani AG. Free vibration of viscoelastic double-bonded polymeric nanocomposite plates reinforced by FG-SWCNTs using MSGT, sinusoidal shear deformation theory and meshless method. Composite Structures. 2015;131:654-71.
[34] Lim C, Zhang G, Reddy J. A higher-order nonlocal elasticity and strain gradient theory and its applications in wave propagation. Journal of the Mechanics and Physics of Solids. 2015;78:298-313.
[35] Li L, Hu Y, Ling L. Wave propagation in viscoelastic single-walled carbon nanotubes with surface effect under magnetic field based on nonlocal strain gradient theory. Physica E: Low-dimensional Systems and Nanostructures. 2016;75:118-24.
[36] Zhen Y, Zhou L. Wave propagation in fluid-conveying viscoelastic carbon nanotubes under longitudinal magnetic field with thermal and surface effect via nonlocal strain gradient theory. Modern Physics Letters B. 2017;31(08):1750069.
[37] Li L, Hu Y. Wave propagation in fluid-conveying viscoelastic carbon nanotubes based on nonlocal strain gradient theory. Computational materials science. 2016;112:282-8.
[38] Ghayesh MH, Farajpour A. Nonlinear mechanics of nanoscale tubes via nonlocal strain gradient theory. International Journal of Engineering Science. 2018;129:84-95.

[39] Farajpour A, Ghayesh MH, Farokhi H. Large-amplitude coupled scale-dependent behaviour of geometrically imperfect NSGT nanotubes. International Journal of Mechanical Sciences. 2019;150:510-25.
[40] Ghayesh MH, Farokhi H, Farajpour A. Chaotic oscillations of viscoelastic microtubes conveying pulsatile fluid. Microfluidics and Nanofluidics. 2018;22(7):72.
[41] Ghayesh MH, Farokhi H, Hussain S. Viscoelastically coupled size-dependent dynamics of microbeams. International Journal of Engineering Science. 2016;109:243-55.
[42] Farajpour A, Rastgoo A, Farajpour M. Nonlinear buckling analysis of magneto-electro-elastic CNT-MT hybrid nanoshells based on the nonlocal continuum mechanics. Composite Structures. 2017;180:179-91.
[43] Ghayesh MH, Farokhi H. Chaotic motion of a parametrically excited microbeam. International Journal of Engineering Science. 2015;96:34-45.
[44] Ghayesh MH. Functionally graded microbeams: Simultaneous presence of imperfection and viscoelasticity. International Journal of Mechanical Sciences. 2018;140:339-50.
[45] Ghayesh MH. Dynamics of functionally graded viscoelastic microbeams. International Journal of Engineering Science. 2018;124:115-31.
[46] Farajpour A, Ghayesh MH, Farokhi H. A review on the mechanics of nanostructures. International Journal of Engineering Science. 2018;133:231-63.
[47] Malekzadeh P, Shojaee M. A two-variable first-order shear deformation theory coupled with surface and nonlocal effects for free vibration of nanoplates. Journal of Vibration and Control. 2015;21(14):2755-72.
[48] Farajpour M, Shahidi A, Farajpour A. A nonlocal continuum model for the biaxial buckling analysis of composite nanoplates with shape memory alloy nanowires. Materials Research Express. 2018;5(3):035026.
[49] Ghayesh MH, Amabili M, Farokhi H. Three-dimensional nonlinear size-dependent behaviour of Timoshenko microbeams. International Journal of Engineering Science. 2013;71:1-14.
[50] Ghayesh MH. Nonlinear vibration analysis of axially functionally graded shear-deformable tapered beams. Applied Mathematical Modelling. 2018;59:583-96.
[51] Ghayesh MH, Farokhi H, Amabili M. Nonlinear dynamics of a microscale beam based on the modified couple stress theory. Composites Part B: Engineering. 2013;50:318-24.
[52] Farokhi H, Ghayesh MH, Amabili M. Nonlinear dynamics of a geometrically imperfect microbeam based on the modified couple stress theory. International Journal of Engineering Science. 2013;68:11-23.
[53] Ghayesh MH, Farokhi H, Amabili M. In-plane and out-of-plane motion characteristics of microbeams with modal interactions. Composites Part B: Engineering. 2014;60:423-39.
[54] Li X, Li L, Hu Y, Ding Z, Deng W. Bending, buckling and vibration of axially functionally graded beams based on nonlocal strain gradient theory. Composite Structures. 2017;165:250-65.
[55] Li L, Li X, Hu Y. Free vibration analysis of nonlocal strain gradient beams made of functionally graded material. International Journal of Engineering Science. 2016;102:77-92.

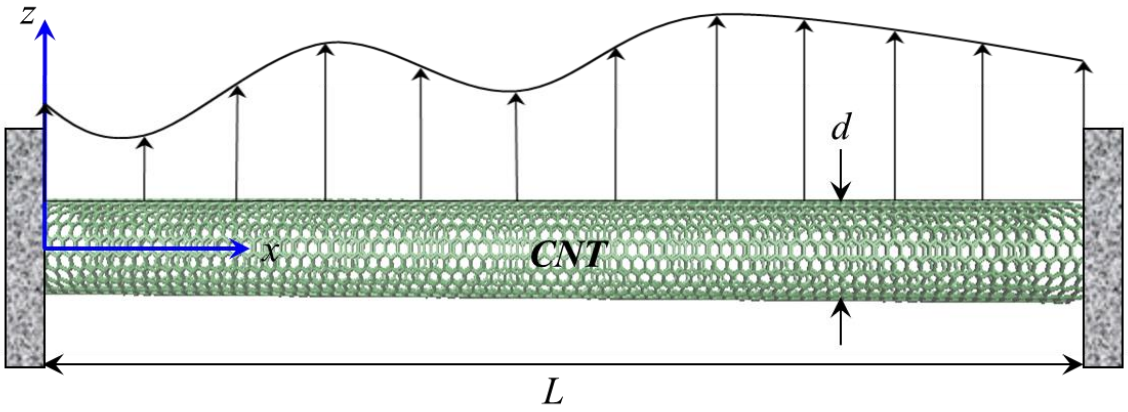

Fig. 1. A coupled viscoelastic CNT under the action of a harmonic distributed force.

(a)

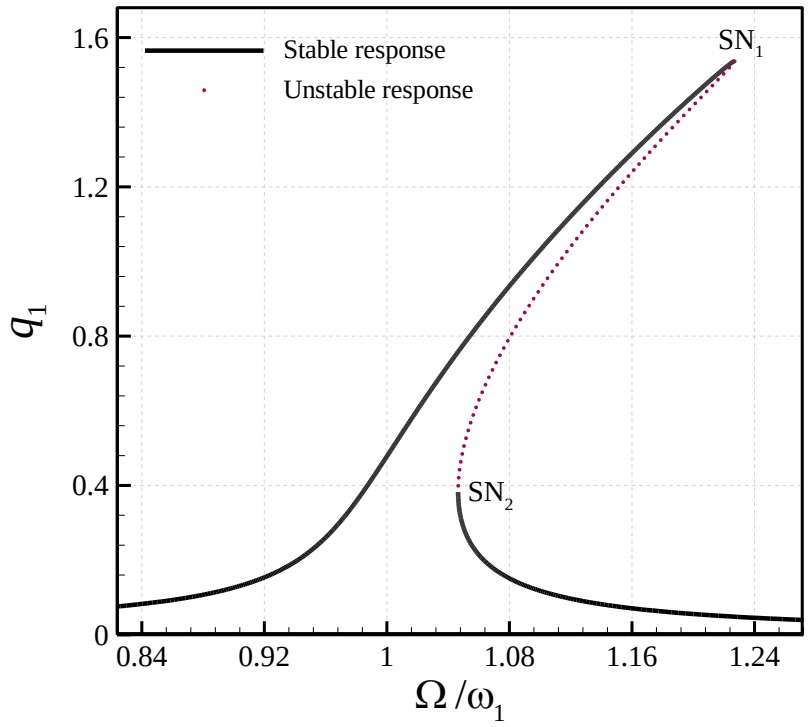

(b)

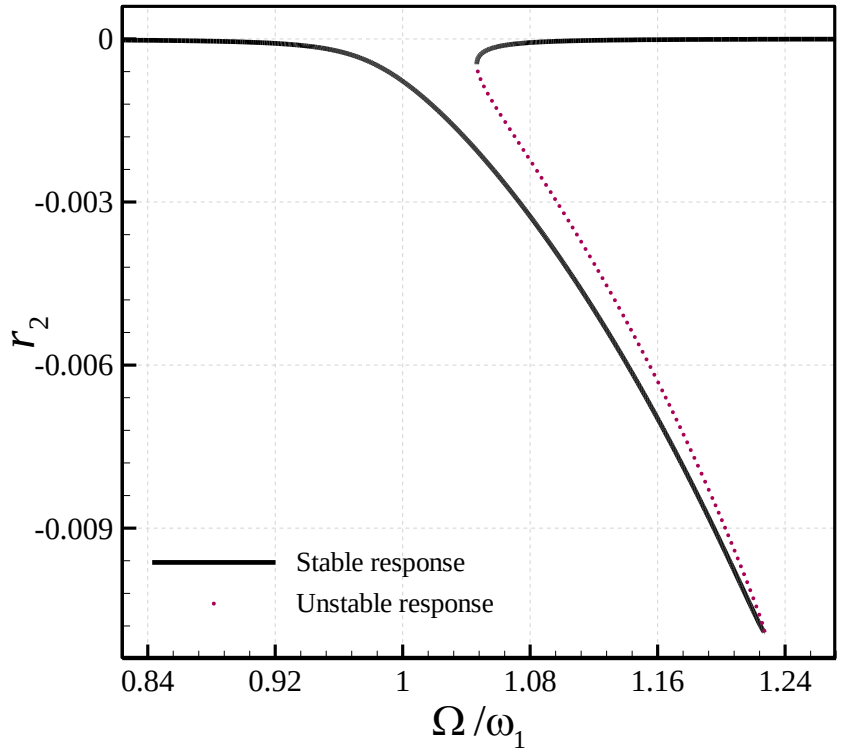

Fig.2. Frequency-amplitude diagrams of the viscoelastic nanotube; (a) the maximum of q_1; (b) the minimum of r_2.

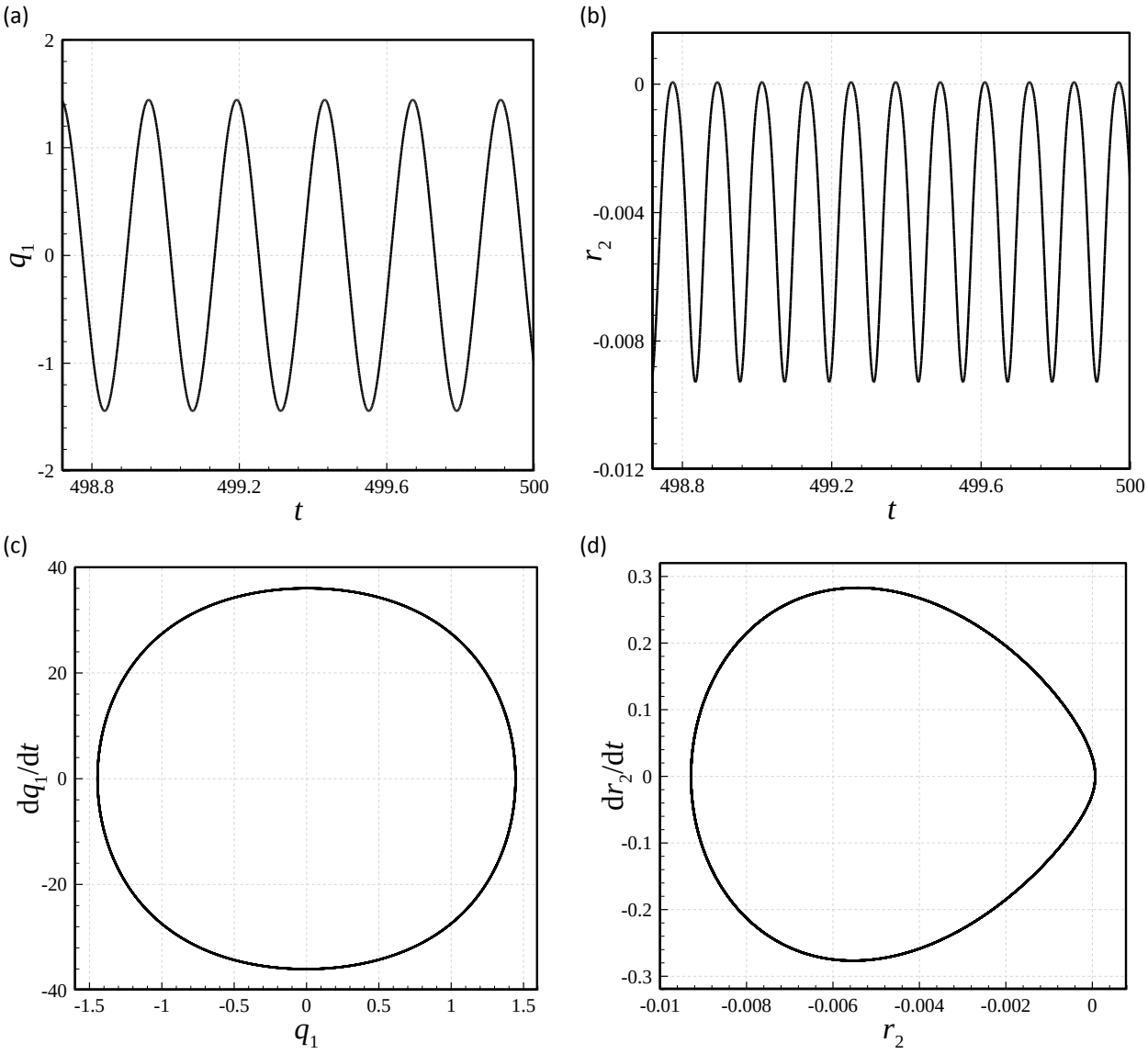

Fig.3. Large-amplitude dynamic characteristics of the viscoelastic nanotube of Fig. 2 at Ω/ω_1=1.20; (a, b) time traces of q_1, and r_2, respectively; (b) phase-plane diagrams of q_1, and r_2, respectively.

(a)

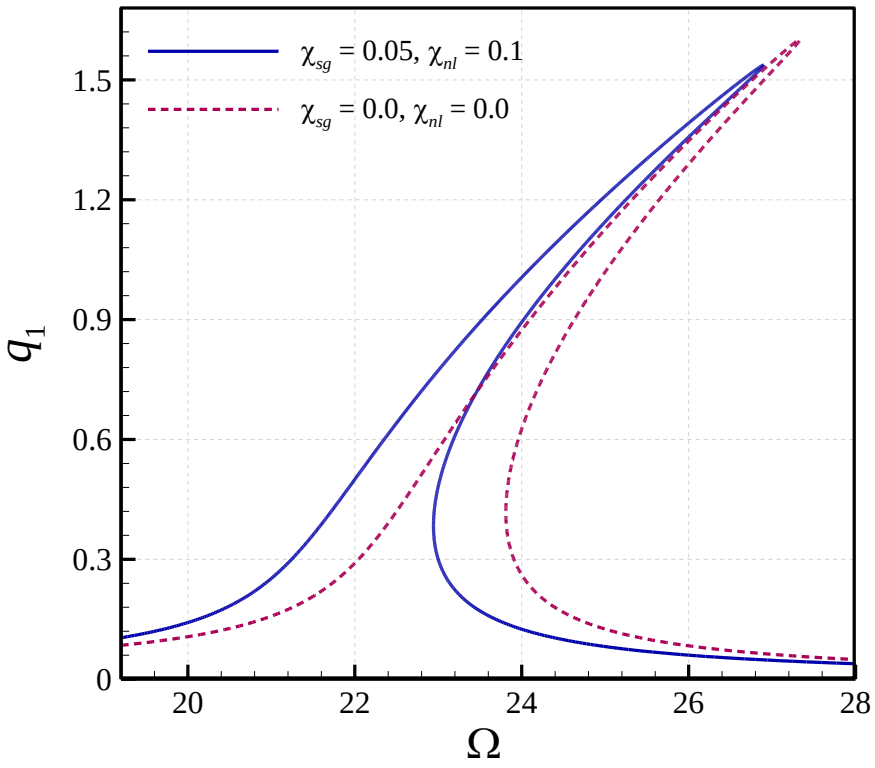

(b)

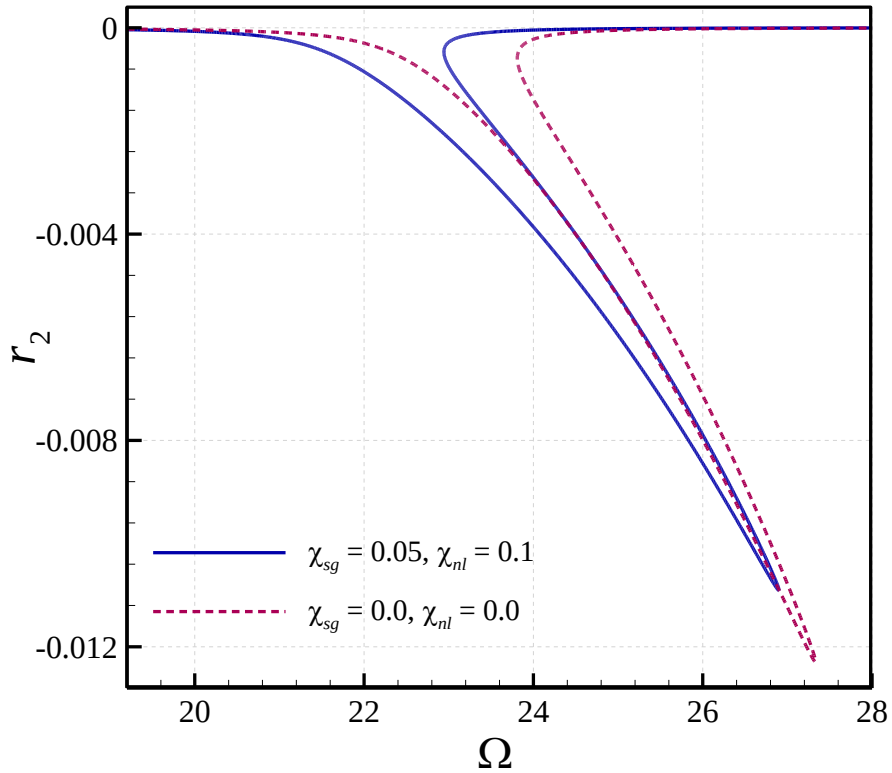

Fig.4. NSGT effects on frequency-amplitude response of the viscoelastic nanotube; (a) the maximum of q_1; (b) the minimum of r_2; F_1=0.30, K_1=20.0, K_2=25.0, and η=0.0005.

(a)

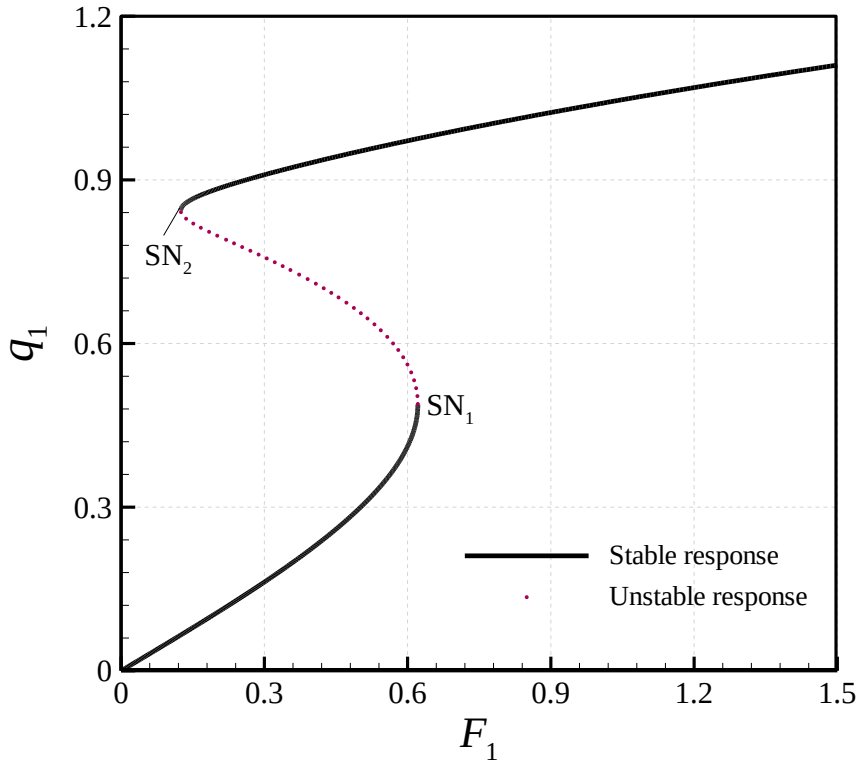

(b)

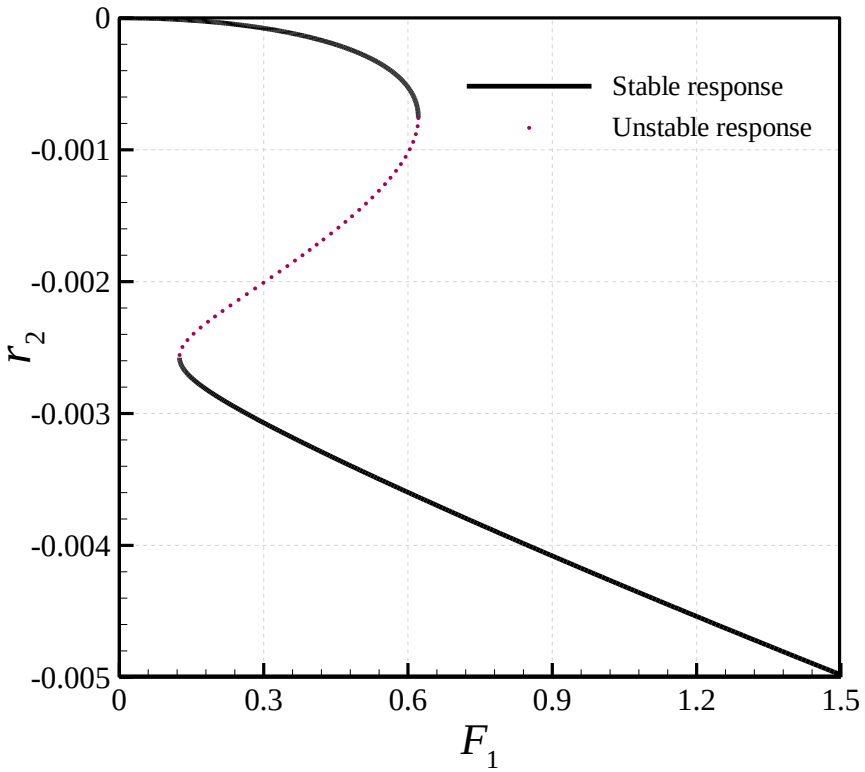

Fig.5. Force-amplitude diagrams of the viscoelastic nanotube; (a) the maximum of q_1; (b) the minimum of r_2.

(a)

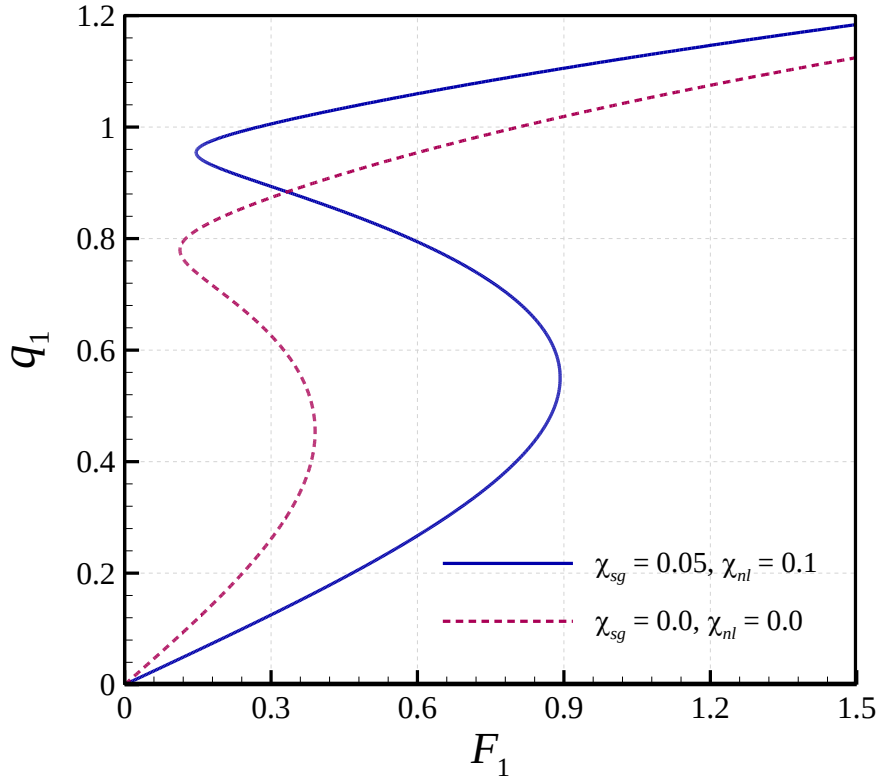

(b)

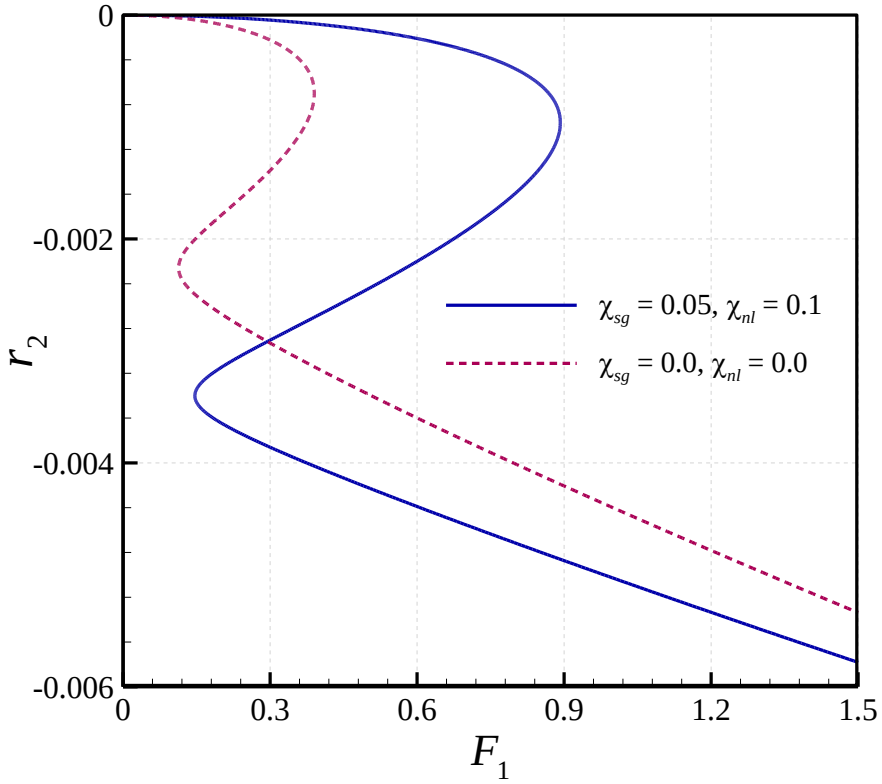

Fig.6. NSGT effects on force-amplitude plots of the viscoelastic nanotube; (a) the maximum of q_1; (b) the minimum of r_2.

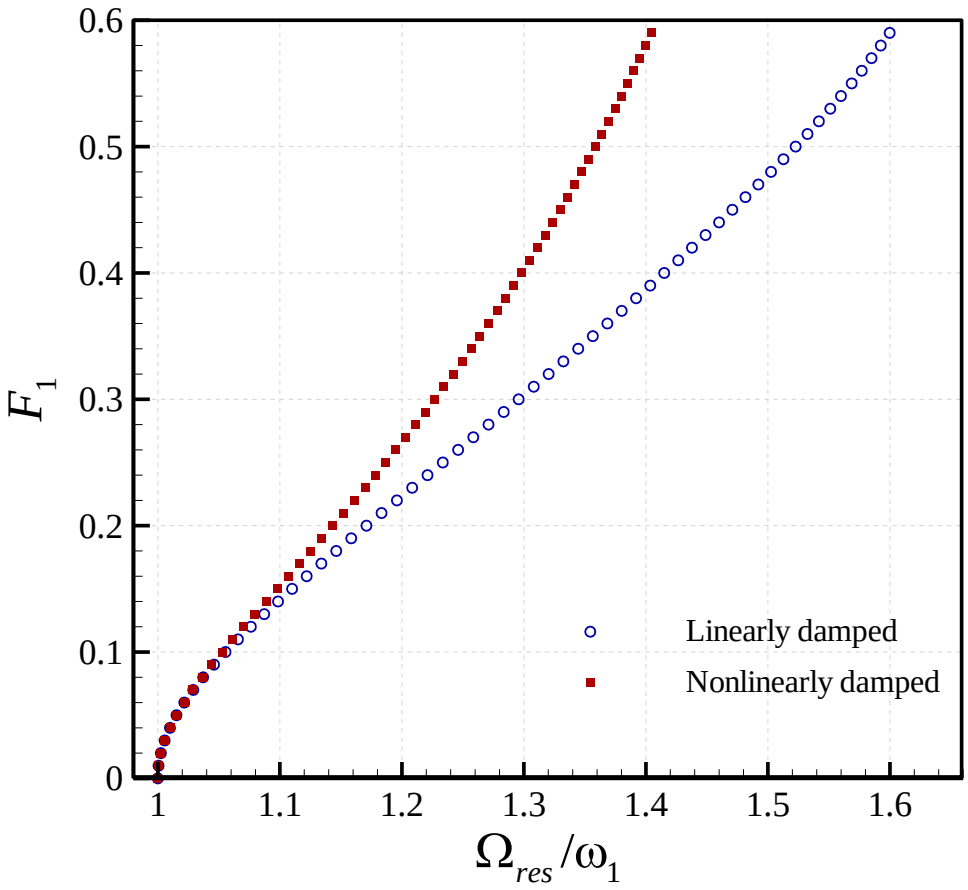

Fig.7: Resonance frequency versus the forcing amplitude determined based on two damping mechanisms; hollow circles show the linear viscous damping mechanism (with ζ=0.006) while solid squares show the Kelvin-Voigt nonlinear damping mechanism (with η=0.0005).

(a)

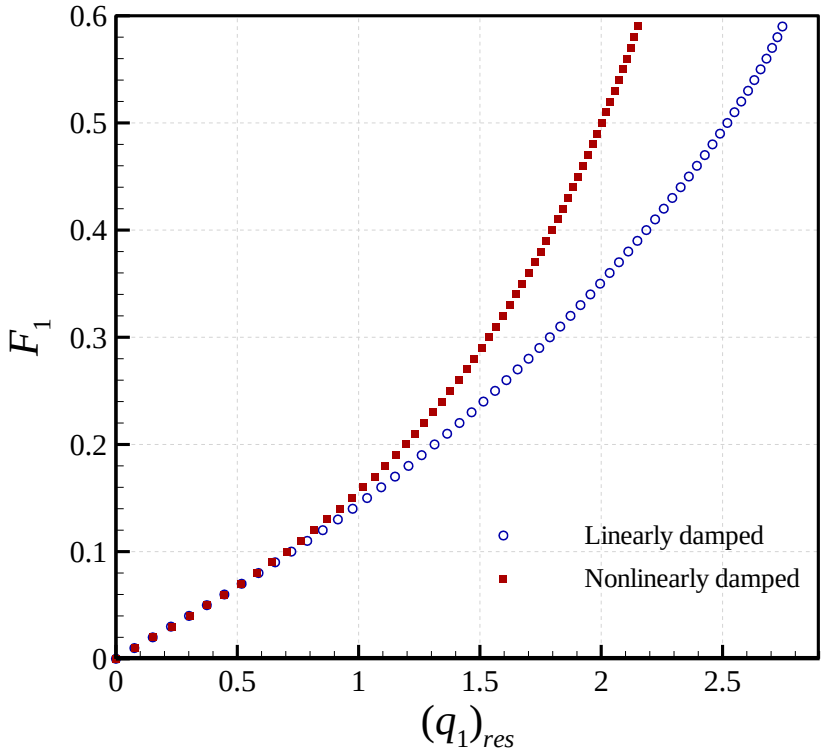

(b)

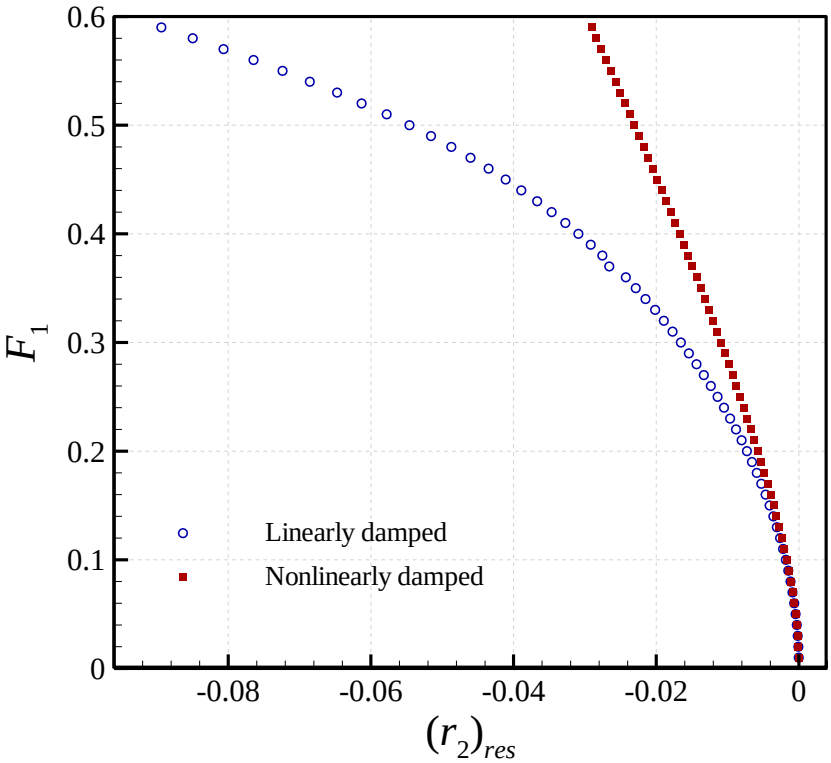

Fig.8: Resonance amplitude of (a) q_1 and (b) r_2 versus the forcing amplitude determined based on two damping mechanisms; hollow circles show the linear viscous damping mechanism (with ζ=0.006) while solid squares show the Kelvin-Voigt nonlinear damping mechanism (with η=0.0005).

(a)

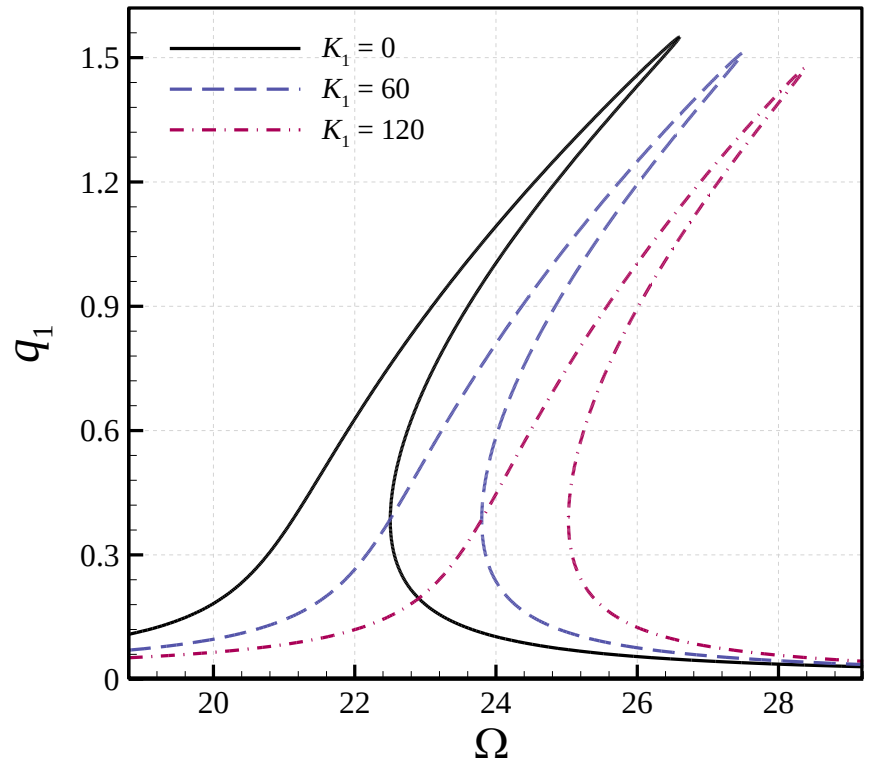

(b)

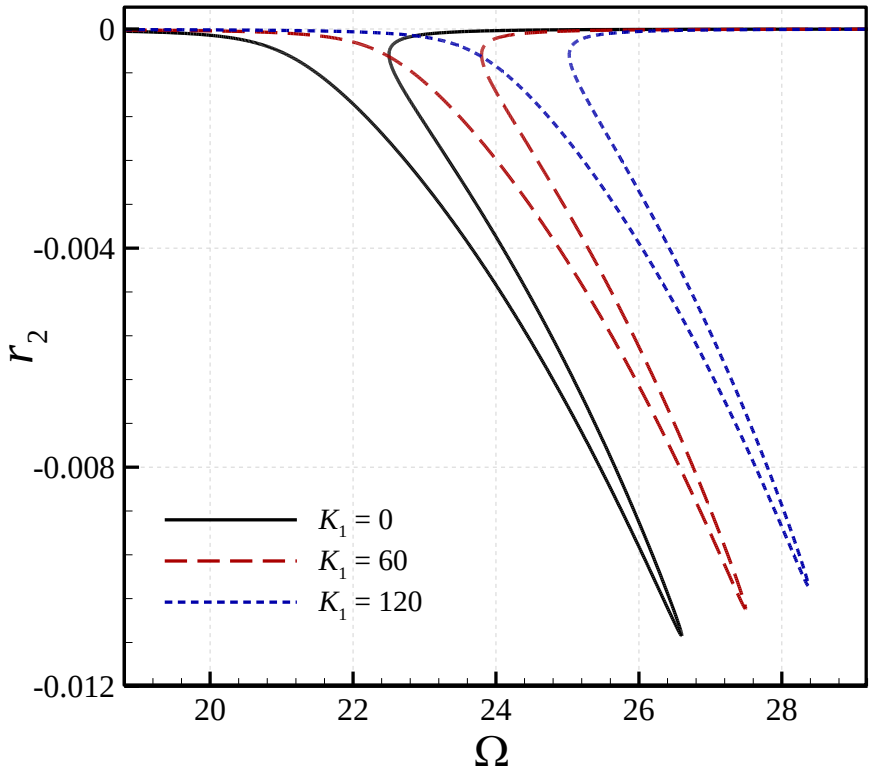

Fig.9. Effect of the linear spring stiffness on frequency-amplitude response of the viscoelastic nanotube; (a) the maximum of q_1; (b) the minimum of r_2; F_1=0.30, K_2=25.0, and η=0.0005.

(a)

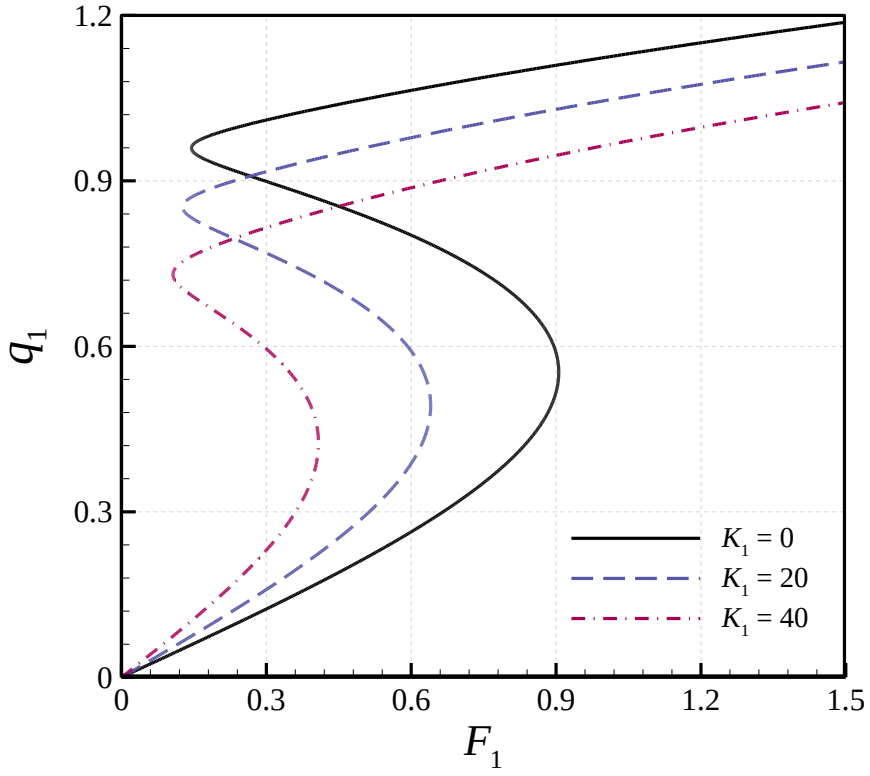

(b)

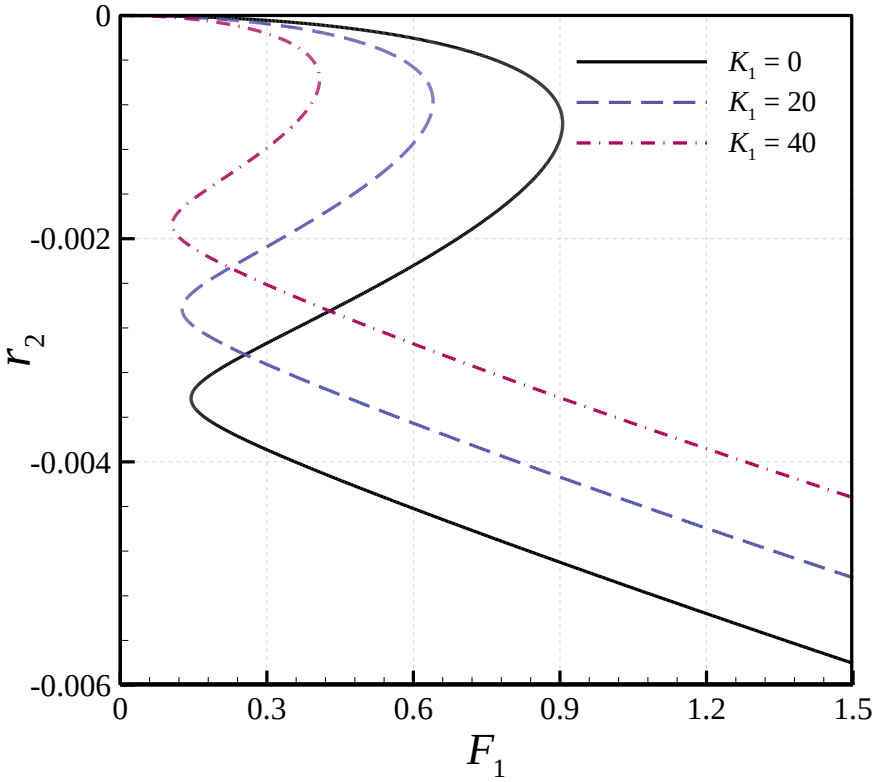

Fig.10. Effect of the linear spring stiffness on force-amplitude response of the viscoelastic nanotube; (a) the maximum of q_1; (b) the minimum of r_2.

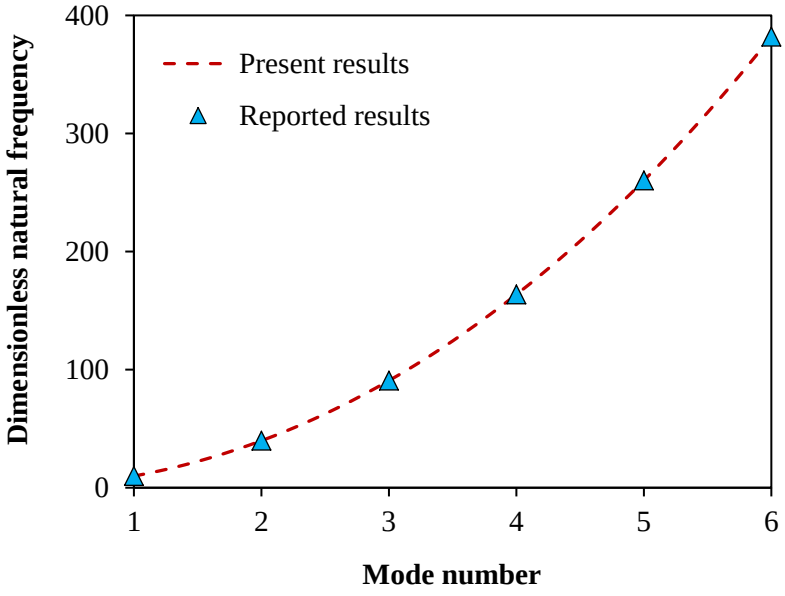

Fig.11. A comparison with the existing results for simply supported nanoscale tubes [54].

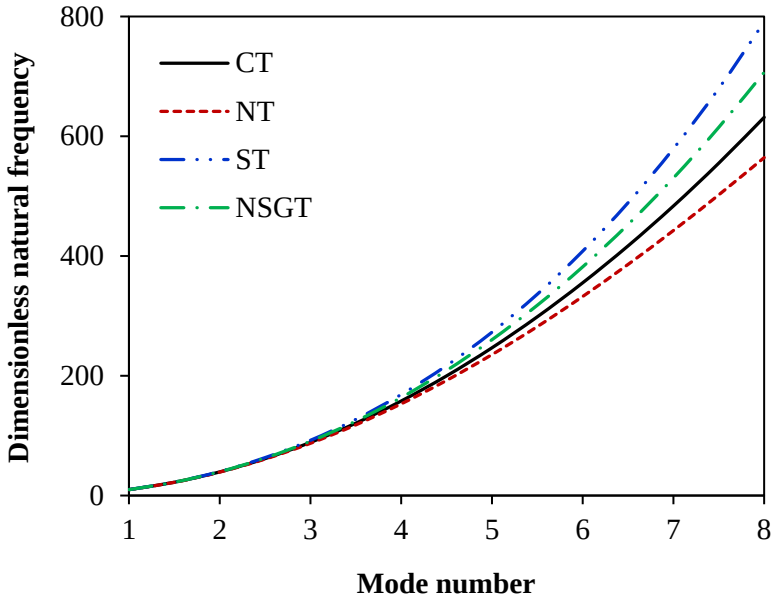

Fig.12. A comparison between different theories for simply supported nanoscale tubes.